Construction and Building Materials 396 (2023) 132289

Contents lists available at ScienceDirect

Construction and Building Materials

journal homepage: www.elsevier.com/locate/conbuildmat

Mechanical properties and microstructural characterization of ferrock as CO_2–negative material in self-compacting concrete

J. Jeffy Pravitha *, R. Ninija Merina, N. Subash

Department of Civil Engineering, University College of Engineering Nagercoil, Tamil Nadu, India

ARTICLE INFO

Keywords:
Self-compacting concrete
Ferrock
Bond strength
CO_2 –negative
Cement–use efficiency index
XRD
SEM

ABSTRACT

The construction industry is one of the major sources of pollution and global warming, with the utilization of cement being a significant contributor. This study aimed to minimize cement usage in construction while maintaining overall strength through the development of sustainable and eco-friendly concrete. A self-compacting concrete (SCC) was created by replacing cement with eco-friendly ferrock, aggregates and super-plasticizers at levels of 5%, 10%, 15%, 20% and 25%. The optimal blend was determined based on fresh and mechanical behaviour parameters. Rheological analysis of the fresh concrete was conducted using L-box, Slump cone, V-funnel equipment and visual stability index. The SCC was then cured through water immersion, CO_2 exposure and a combination of both. The performance of the ferrock SCC was evaluated under different curing conditions to determine its hardened and microstructural properties. The addition of ferrock altered the properties of the concrete, and changing the curing method also influenced the behaviour of the hardened concrete. CO_2 curing achieved about 40% of the concrete strength within four hours, while combined water and CO_2 curing produced higher-quality concrete, as shown by UPV, SEM, and XRD results. The incorporation of ferrock almost doubled the strength of the concrete in combined curing. At an optimum replacement level of 10%, the compressive strength values of water, CO_2, and combined curing increased by 21.9%, 25.9% and 32.6%, respectively, after 28 days. The bond strength also increased by 20% at this level of ferrock addition for combined curing. Comparison with normal SCC indicated that the ferrock-based SCC was physically stronger at an optimum replacement level of 10%, with a higher degree of compaction and dense matrix. These findings suggest the superiority of ferrock SCC, which offers potential for use in future construction.

1. Introduction

The activities of the construction industry have almost reached its peak in recent decades and the heights of buildings are increasing at a large pace every day. In such an event, the usage of normal concrete is fairly difficult for being compacted at heights. Also, in the case of narrow beams or where there is less working space normal concreting has become tedious [1,2]. In such a situation, SCC can eliminate the issue faced in the compaction of concrete in high-scrap buildings. Besides, it minimizes the duration of construction. The concept of self-compacting concrete came into being in the late 1980s, offering good flowability and ideal compaction under its self-weight [3]. Owing to its advantages, its application spreads widely in the construction of dams, bridges, high-rise buildings and infrastructures.

Contrary to the claim, the utilization of SCC in the construction industry has to deal with a large quantity of portland cement and chemical substances imposing limitations on the sustainability of concrete technology. This issue can be solved by recycling industrial byproducts to maintain the freshness and durability of the concrete [4–6]. Also, the world's thirst for materialization and industrialization is increasing in an alarming way increasing carbon intrusion into the atmosphere. The construction sector accounts for the emission of 38% of carbon forming a reason for climate change, says the UN report [7] which compels researchers to look for a suitable carbon-negative material. One such material is ferrock, developed from the combination of industrial residues with an absolute capacity of absorbing CO_2 in the air like a sponge. It is a less expensive material developed by researchers equal to that of Portland cement concrete having ideal mechanical and flexural properties [8].

Ferrock is a combination of iron dust, fly ash, metakaolin and limestone powder with a major proportion of iron scraps from steel industries [8,9]. In recent times, India has become the second-largest

* Corresponding author.
E-mail address: jeffypravitha@gmail.com (J. Jeffy Pravitha).

https://doi.org/10.1016/j.conbuildmat.2023.132289
Received 10 February 2023; Received in revised form 16 June 2023; Accepted 23 June 2023
Available online 6 July 2023

sector of steel manufacturing in the world. The global production of such a demanded material is fully yielded by several steel units all over the country. The ministry of steel in India reported a huge turnover of 99.57 million tonnes of steel around the global year 2020–2021. In such a scenario, environmental management and energy efficiency becomes the crucial elements to be under control to balance environmental destruction [10]. In favour, the ministry of steel has offered the possible use of slag waste from the iron and steel industries in the construction department with the provision of developing codes and guidelines for landfilled hazardous materials. Eventually, the increase in the iron and steel market expected a dropout of 2,40,643 tonnes of mill-scale waste, iron dust and other solid wastes into the dry lands [11]. These scraps occur either as metallic iron or as iron oxides in the form of wustite (FeO), haematite (Fe_2O_3) and magnetite (Fe_3O_4) [12,13]. It is as well associated with iron specks of dust which were liberated during the fume purification process with a copious amount of iron oxide in it [14]. These residues can harmfully spoil the soil morphology of the dumped areas. As a matter of recycling the above, researchers have utilized them as replacements in concrete and acquired satisfactory results. Partial replacement of iron particles for cement has been reported, which states the traces of silica present in the iron slag is converted to calcium silicate and aluminate which serves as an activation factor in filling the voids through the interfacial transition zone (ITZ) of the concrete.

The SEM studies of the above concrete showed a well-developed crystalline structure along with ettringite causing a denser matrix with iron slag [15]. Moreover, studies have been extended to analyze the degree of durability issues while incorporating iron in concrete. The iron-filled SCC performs relatively well in acid and sulfate exposure with good resistance to chloride ions [16]. Besides its solid nature, the iron fillings gave greater strength to the concrete due to its angular texture which actively fills the voids thereby enhancing the mechanical properties [17]. Studies have also proved the material greenness of these iron-packed engineered composites in minimizing primary energy usage and CO_2 emission [18]. Additionally, the pozzolanic materials in ferrock concrete like fly ash, metakaolin and micro sized limestone powder enhanced the filling effect in the concrete and build a better bond between the aggregate and the cement paste [19–23]. Equally, the addition of 10% silica fume in SCC does not find to hinder the performance of concrete but instead helps in maintaining the flow partially [24]. On concern with flowability, researchers focused the potential use of superplasticizers (SP) and viscosity modifying agents (VMA) in SCC, which assist in maintaining the fluidity and stability of concrete, consequently reducing bleeding and segregation problems [25]. This increases the ease of working and prevents the problem of the aggregates get clogging between the reinforcement [9].

The well-settled idea of using pozzolanic materials in concrete is needed to be revisited in the context of utilizing industrial waste materials and byproducts such as iron dust, fly ash, metakaolin and limestone powder in the form of ferrock in SCC. Furthermore, ferrock is an old revolutionary material entirely composed of waste materials, its use is restricted in the construction industry owing to its less affordability for large scale projects. One of the alternatives for rehabilitating the ferrock technology is blending this source material with cement and finding the possibility of curing without external CO_2 sequestration. The study aims in the aforementioned statement by finding the optimum replacement of ferrock in SCC to compromise the concrete strength and to analyze the feasibility of preparing ferrock-based SCC without CO_2 curing. This paper presents a novelty of finding an economic method of repurposing the thrown out hazardous by products from industries in the form of ferrock to develop an environmentally friendly high strength self compacting concrete which can possibly be the futures' preference.

The ferrock, developed by David Stone is purely a non-cement material which hardens by the carbonation of pozzolanic materials in the presence of oxalic acid. The chemical reaction between iron dust and CO_2 yields iron carbonate which initiates the strength of the ferrock concrete [8,26]. The present study tries to incorporate this eco-friendly material in combination with cement and analyses the feasibility of developing a hybrid ferrock concrete under water curing. The behavior of ferrock in SCC under different curing regimes was studied. The influence of ferrock on the flow characteristics of the fresh SCC and the hardening phenomena of the concrete formed part of the study. Microstructural characterization was carried out to evaluate the porous nature of the concrete matrix and the bonding of the aggregate-cement mortar. The compatibility of ferrock with SCC under conventional and non-conventional methods of curing was studied and the optimum percentage of ferrock with satisfactory results were reported.

2. Materials and methods

2.1. Materials

The cement used is OPC grade-53 with a specific gravity of 3.15 and a fineness modulus of 5% on 90μ sieve, conforming to the standards of BIS 12269 [27]. The oxides and phase mineralogy composition were identified by XRF (Table: 1) and the SEM and XRD data analysis were as shown in Fig. 1. The calcium content is greater than 60%, comprising alite and belite crystals with traces of silicate and aluminate. The SEM images an irregular rough texture of cement particles as seen in Fig. 1.

Ferrock is a complex material comprising iron dust, fly ash, metakaolin and limestone powder. Required iron dust was collected from an iron & steel industry from Karnataka (India), where its disposal is reported to be difficult and cost-intensive. As the above material was sourced from the disposal yard, the size of the particles was not uniform which necessitated screening in the sieve (90 μ). The ferrock is then prepared using 60% iron dust 20% fly ash, 10% limestone and 10% metakaolin. The cumulative particle size distribution as analysed by PSA (particle size analyzer) gave a mean particle size of 75 μm (Fig. 4), which correlates the compatibility of ferrock micro-particles with that of cement. The fly ash used here is of class F with specifications conforming to BIS: 3812-1987 [28] and the limestone and metakaolin were of size less than 100 μm. The oxidal composition is presented in Table 1. The structural composition of minerals in ferrock was analyzed by X-ray diffraction (XRD) conducted at 2θ in the range of 10° to 80° and the peak mineral components were identified. The sharp narrow peaks characterize the crystalline phases of hematite (Fe_2O_3) and aluminium-bearing hematite ($Fe_{1.84}Al_{0.16}O_3$). The analysis also confirmed the presence of diopside [$Ca_{0.59}Mg_{1.41}SiO_6$], andradite ($Ca_3Fe_2SiO_4$) and *meta*-sillimanite (Al_2SiO_5) as major components. The surface morphology and mineral phase distribution of ferrock (Fig. 2) confirm the occurrence of iron oxide as a major component constituted by small-sized particles with high surface area [29,30]. Iron oxide is a naturally occurring compound that can exist in several forms, including hematite, magnetite, and goethite. These forms of iron oxide have distinct crystal structures and exhibit characteristic peaks in their X-ray diffraction patterns. Therefore, the presence of iron oxide in a material can result in a narrow peak configuration that is indicative of a highly crystalline material [31]. On the other hand, the calcite, silicate and aluminate phases are minerals that typically have less well-defined crystal structures. These phases can exist in various forms, including amorphous or poorly crystalline, which can make the material appear more amorphous overall. Therefore, the combination of these two types of phases in a material can result in a material that exhibits both highly crystalline and amorphous properties. This can make it challenging to characterize the material accurately, as it may exhibit a mixture of narrow and broad peaks in its X-ray diffraction pattern. Overall, the presence of iron oxide may contribute to a narrow peak configuration, but the other phases present can make the material appear more amorphous in nature.

The silica fume with an average particle size of 25 μm is used in this study (Fig. 4). The PSA showed a cumulative diameter ranging from 4.2 μm (10%) to 54 μm (90%). XRD results in Fig. 3 display the SiO_2 content in the form of quartz, which accounted for a high percentage followed by traces of MgO, K_2O and Na_2O (Table 1).

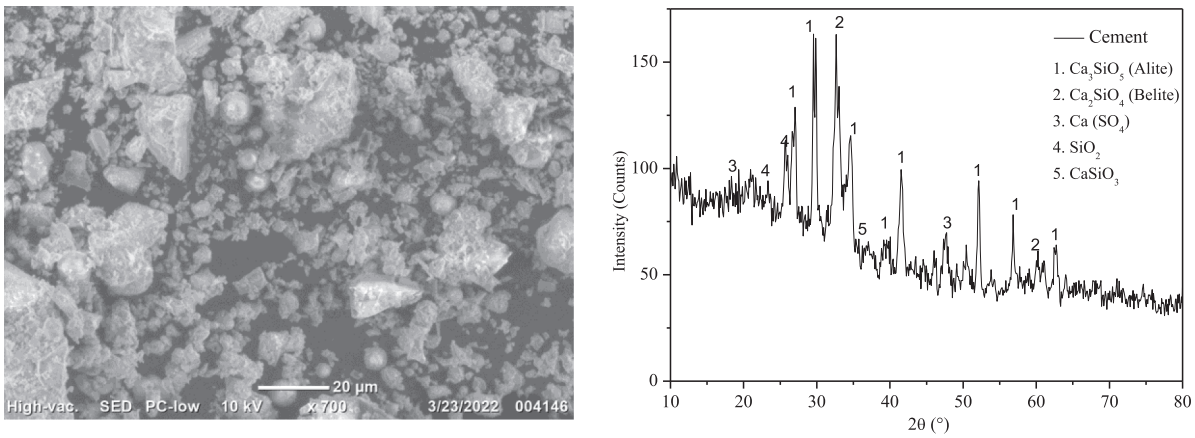

Fig. 1. SEM and XRD data for cement.

Table 1
Oxide composition in percent of cement, ferrock and silica fume.

Oxide	Cement	Ferrock	Silica fume
CaO	68.05	6.50	2.05
SiO_2	17.51	27.23	86.85
Al_2O_3	9.75	20.88	1.88
MgO	2.59	11.22	1.28
Fe_2O_3	–	32.66	1.88
SO_3	–	0.04	0.90
Na_2O	1.22	0.56	1.00
K_2O	0.88	0.22	4.30
TiO_2	–	0.69	\mathord{-} -

Also, good quality manufactured sand from rock dust (M-sand) of size below 4.75 mm was used as a fine aggregate. As high as 96% of the above sand particles passed through 4.75 mm sieve. The specific gravity was determined to be 2.26 and the fineness modulus was 3.31 conforming to zone II of IS 383–1970 [32]. Coarse aggregate of crushed granite to a maximum size of 12 mm was used. The specific gravity and fineness were 2.56 and 6.5 respectively in accordance with IS 2386 (Part I)-1983 [33]. The grading of the aggregates was presented in Fig. 4.

The superplasticizer used in this study was a poly-carboxylate based ether (PCE) with a specific gravity of 0.02 to 1.10. PCE is a new generation polymerized superplasticizer conformed to BIS: 9103:1999 [34], with a high molecular weight that performs superior to other water retarders in maintaining the slump at the usual setting time of the concrete [35]. The viscosity modifying agent used was also a polymerized form of poly-carboxylate ether solution obtained locally from a chemical manufacturing industry. It was a colorless to light hazy liquid with a pH of 6 and a specific gravity of 1.10. Normal tap water was used for the mixing.

The calculated quantity of the components was mixed to get ferrock-based SCC to qualify for EFNARC standard [36]. Despite the existence of some standards, it is more important to conduct some tests on several trails in order to improve component ratios and rheological standardization for filling and segregation. For a high strength, self-compacting concrete of grade M40, a combination in the proportions 1:1.27:1.32 was developed. Table 2 indicates the replacement level of cement with ferrock. Ferrock was substituted at different levels (5, 10, 15, 20 and 25%) of cement with a control mix. Silica fume was substituted at a constant level of 10 % of cement in all mixes. The water-to-binder ratio was kept at a constant range of 0.32 with a fine aggregate content maintained within the specified limit of 48–55% of the total aggregate [36]. The volume ratio of paste to the concrete mixture was 0.42 and the paste content in the mix was 409.5 l/m^3. Generally, SCC is developed with high powder content at a low water/cement ratio [37] for which the flowability is achieved by the addition of superplasticizers and viscosity modifying agents. The superplasticizer used was 1.5% of the binder content and water content (190 ± 10 l/m^3) and was marginally adjusted to achieve the performance of the fresh mix.

The mixing was done as follows: The components in dry form were mixed well using a mixer machine for one minute. Around 70% of the

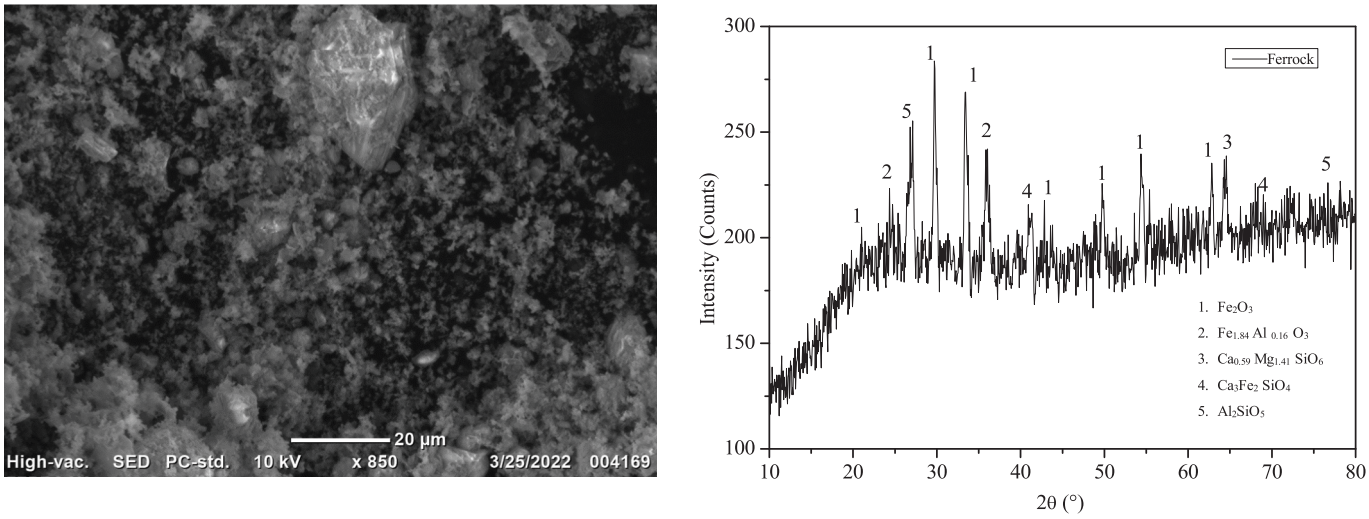

Fig. 2. SEM and XRD data for ferrock.

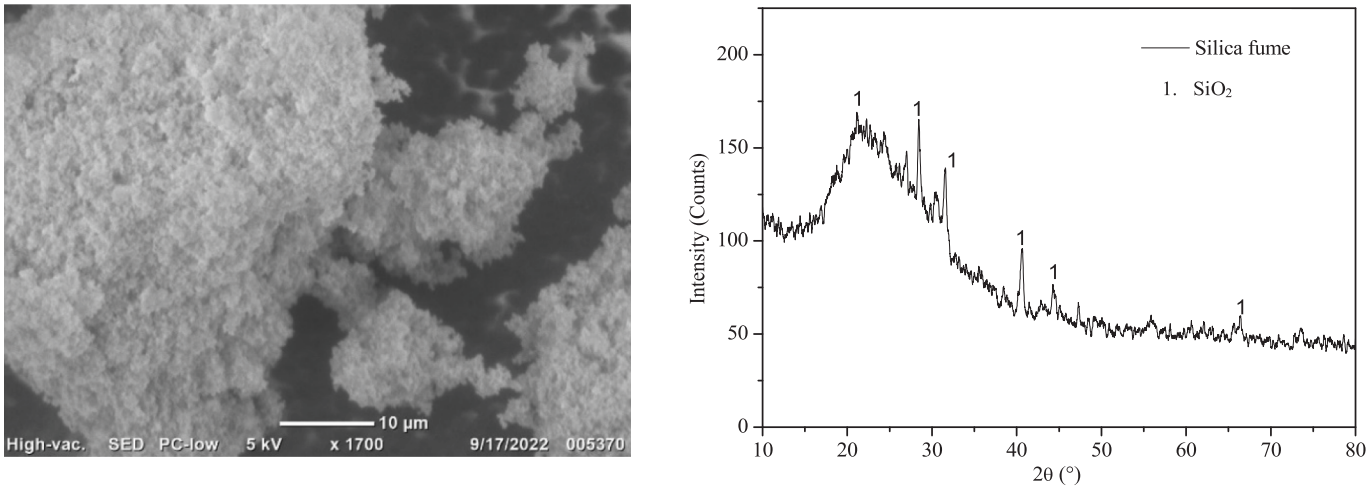

Fig. 3. SEM and XRD data for silica fume.

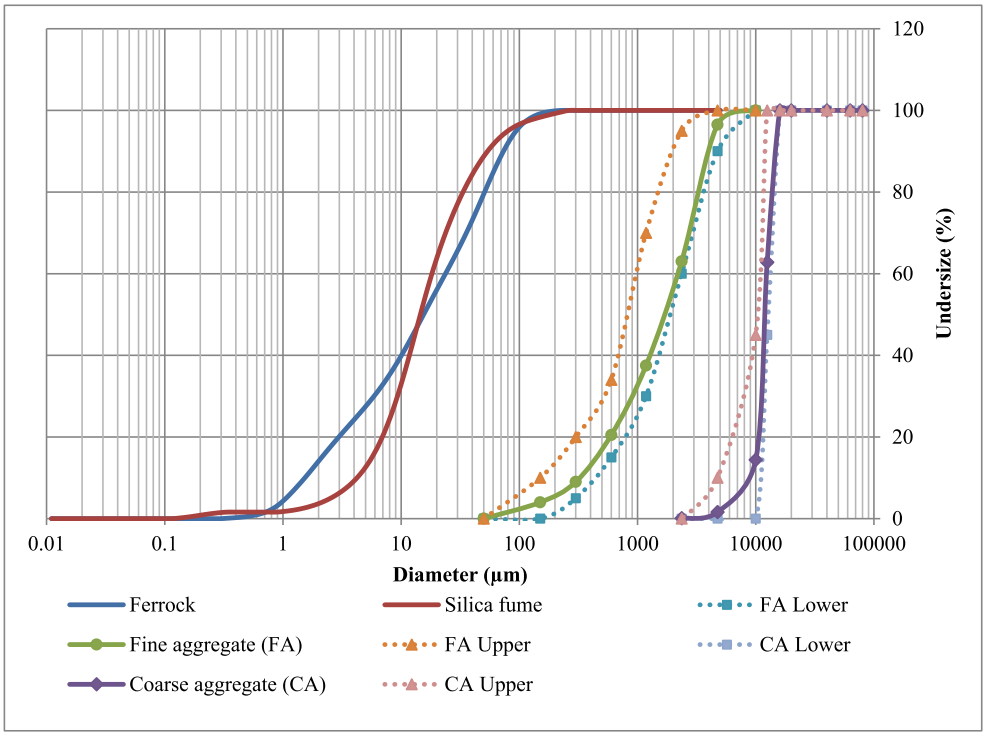

Fig. 4. Particle size distribution of ferrock, silica fume, and fine and coarse aggregates used in the study (upper and lower limits of fine and coarse aggregates corresponds to IS 383-1970).

Table 2
Material Composition of SCC.

Mix ID*	Cement (Kg/ m^3)	Silica fume (Kg/ m^3)	Ferrock (Kg/ m^3)	Fine aggregate (Kg/m^3)	Coarse aggregate (Kg/m^3)	Water (l/m^3)	SP (%)	VMA (%)
SCCF0	550	50	0	764	790	180	1.5	0.1
SCCF5	522.5	50	27.5	764	790	180	1.5	0.1
SCCF10	495	50	55	764	790	186	1.5	0.1
SCCF15	467.5	50	82.5	764	790	190	1.5	0.1
SCCF20	440	50	110	764	790	196	1.5	0.1
SCCF25	412.5	50	137.5	764	790	200	1.5	0.1

*SCCF0 represents the control mix and SCCF5, SCCF10, SCCF15, SCCF20, SCCF25 represent ferrock-SCC at 5, 10, 15, 20 and 25% respectively.

total water required is then added and mixed for another minute. Superplasticizer is added to the concrete mixture with the remaining 20% of water [21]. Finally, the remaining 10% water and viscosity modifying agent were added and blended with SCC. The SCC thus prepared is tested for its workability requirements and then cast into cubes with the side measurement of 150 mm and cylinders (150 mm dia. and 200 mm height). The fresh SCC poured into moulds was placed under ambient room temperature for one day to enable the setting. After 24 h, they were unmoulded and subjected to three different curing conditions.

- C1 curing by hydration with a relative humidity of 100 %, for 7,14,28 and 56 days
- C2 curing in a closed environment containing CO_2 at an initial pressure of 340–380 kPa [38] for 4 h followed by air curing under ambient temperature for 7, 14, 28 and 56 days.
- C3 curing under CO_2 for 4 h with similar conditions of C2 followed by water ponding until 7,14,28 and 56 days of testing.

The CO_2 curing was carried out in a closed chamber with an outlet valve and an inlet pressurized valve for the supply of CO_2 and its regulation. The demoulded SCC specimens were kept in a sealed chamber containing CO_2 gas of 99.9% purity and the gas is allowed to penetrate the samples under high pressure of about 350 kPa (350 ± 10 kPa). After 4 h the samples were taken out of the chamber and exposed to the above mentioned curing conditions.

2.2. Methods

2.2.1. Test setup and procedures

The rheological study on the passing and filling ability of the viscous SCC characterizes the flowability criteria. Slump test, T500, V- funnel, V-funnel at $T_{5\ min}$ and L-box test were carried out as per IS 1199 part 6 [39]. Also, visual observation was done to assess the possibility of segregation and bleeding in concrete. Also, concrete in its hardened state was tested for compression, tension and density to assess the robustness under differential curing regimes. Three cubes of the size 150x150x150 mm were compressed under a Universal Testing Machine (UTM) according to IS 516 (1959) [40] and the average ultimate strength was evaluated. Similarly, cylindrical specimens were tested under UTM for tension along the horizontal axis as per IS 5816 (1999) [41]. An Ultrasonic Pulse Velocity test was also carried out in accordance with ASTM C 597-02 [42], to infer the porous nature and quality of the solid concrete material.

The Bond test is done in accordance with RILEM RC6 [43]. Pull-out specimens are customized by supporting a 16 mm reinforced rod to the full depth of the cube specimen through its vertical axis. After 28 days of relevant curing, the pull-out specimens are tested under UTM and the nominal bond strength τ_{bond} was determined [44,45] using the Eqn. (1):

$$\tau_{bond} = \frac{F_{max}}{\pi dl} \tag{1}$$

In exercising the above formula, it is assumed that the distribution of bond stress along the embedded length of the steel bar was uniform. Here the value 'l' was kept constant for every mix specimen as 150 mm.

2.2.2. CO_2 uptake and cement-use efficiency

The quantity of CO_2 absorbed was estimated as per the mass-curve method [38,46]. Eqn. (2) is used to know the degree of carbonation for the CO_2-exposed samples by proportioning the mass increment on the samples. The change in mass directly correlates to the amount of reacted CO_2.

$$CO_2\ \text{uptake}\ (\%) = \frac{M_f}{M_i} \times 100 \tag{2}$$

In the above equation, M_f denotes the increase in mass of the sample subjected to CO_2 whereas M_i, is the initial mass of the sample. Cement-use efficiency index calculation is made to arrive at the reduced usage of cement in ferrock-based SCC production. Eqn. (3) calculates by determining the total amount of binder necessary to develop 1 MPa of strength [47,48]. The SCC performance based on this index serves as the deciding factor for satisfactory surveillance of ferrock in a hazard free environment.

$$C_i = \frac{b}{p} \tag{3}$$

Where, C_i- cement use efficiency Index, b- the total amount of cement consumed, p -performance of the system which is mainly compressive strength.

2.2.3. Micro-structure characterization

Broken concrete pieces were crushed to powder and sieved in a 90-μm sieve. A sample containing 5 g was tested in an X-Ray Diffractometer at a range of diffraction angle (2θ) between 10° and 90° with a step width of 0.02°. The XRD spectral patterns obtained are then analyzed by comparing the peaks with the JCPDS chart of inorganic compounds. For morphological analysis, a high-vacuum scanning electron microscope with secondary electron detectors was used at 10 kV, picturing the mineralogical components formed during the process of hydration and carbonation.

3. Results and discussions:

3.1. Fresh concrete analysis

The firmness and the viscosity of flow determine the stability of SCC which is characterized from the fresh concrete examination by slump test, T500 test, V – funnel and L – box tests. Visual observation on segregation and bleeding was done to avoid deformability and the high risk of drying shrinkage in concrete. The amount of water added to an SCC mix impacts the workability of the concrete in a number of ways [19]. Since ferrock is relatively a water-absorbing firm [49], estimated slump flow diameter was designated to a maximum limit (725 mm), which would not likely affect the flow with the addition of ferrock. On enquiring about the slump specifications, all the values fall under the slump class of SF2, where EFNARC suggest a safe applicable limit for the normal construction of walls and columns [36]. Upon addition of ferrock, the slump flow was found a whit restricted as expected, although resilient in its properties against 25% replacement of ferrock as shown in Fig. 5. Each increment in ferrock content decreases the slump rate by an average of 10 mm as the iron powder in ferrock retards the flow rate of the fresh mix, whereas the presence of fly ash, metakaolin and limestone powder was found to increase the working ability in its fresh state [50]. These ultra fine particles tend to fill the voids existing among the binder particles, thereby decreasing the ratio of voids between the cementing substances. It can be said to balance the water content absorbed by the iron powder [51]. Furthermore, the existence of limestone in the supplementary material creates a positive synergetic action with the fly ash promoting the liquid state behavior of SCC due to its structural configuration and filling capability [52,53].

L-box test values were defined in the range of 0.8 – 1 [36]. All the mixes with ferrock have been found to possess its marginal distribution of values between the limits except SCCF25 as in Fig. 5. However, it was suggested to have the L-box values from 0.6 to 1, as a criterion of blocking resistance necessitating passing ability [54]. Thus, all the SCC mixes can be accepted for its satisfactory performance under the filling and passing ability. The viscosity of the mix is remarkable by its perception under T500 and V-funnel tests. Fig. 6 reveals a drop in flow seconds indicating an impingement in filling ability for higher replacement of ferrock. Such hindrance may be due to the high-level packing density of minerals which would progressively lower the rate of flow in the mix [55]. The flow concerning plastic viscosity is smooth up to 15% replacement of ferrock, thereafter the flow rate tends to outrage the

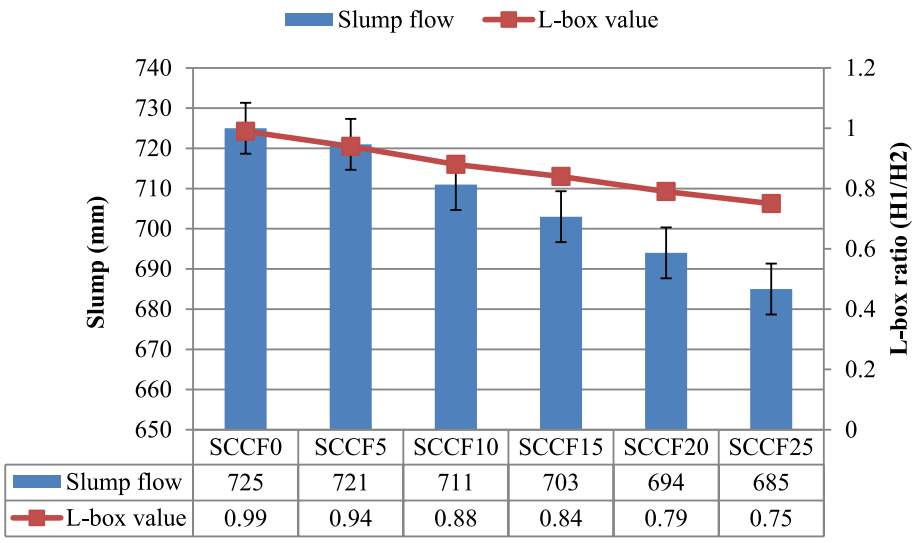

Fig. 5. Influence of ferrock on the properties of slump and L-box ratio (Slump flow of 660–750 mm is maintained which notifies class of SF2 according to EFNARC).

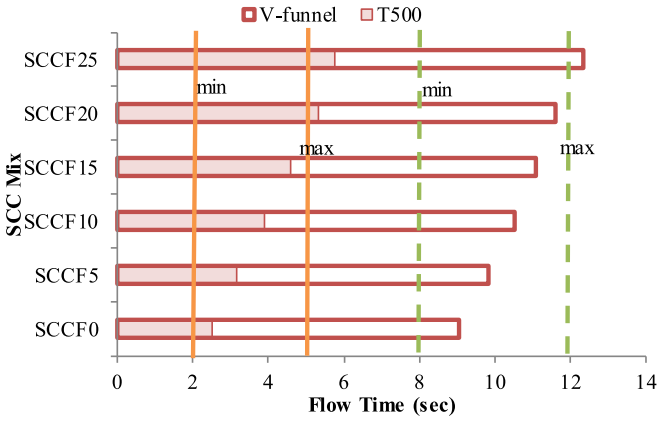

Fig. 6. Influence of ferrock on the properties of T500 and V-funnel time.

limitations specified by EFNARC [36]. The addition of fines tends to increase the viscosity of the mix, thus decreasing the flow rate followed by an increased time of flow which is in agreement with earlier works [50,56].

The segregation was analyzed by visual stability index (VSI) and V-funnel at $T_{5\ min}$ and the values are given in Table 3. Mix SCCF25 demonstrated an unsatisfactory time of flow, besides the mix looked unstable with a minimal threat of segregation and bleeding, which falls under the category of VSI I. All the other mixes were found to have an acceptable performance of + 3 sec in $T_{5\ min}$ and incurred a visual stability index of VSI 0. The discrepancy is due to an increase in plastic velocity that gradually decreases the settlement rate of coarse aggregates improving the property of segregation resistance [4]. The relationship between bulk density and fluidity in concrete is apparent, as a higher bulk density results in a lower rate of fluidity. However, the addition of pozzolanic fines with a ball-bearing effect can increase the rate of flow by reducing cohesion between particles, which may lead to segregation and bleeding in self-consolidating concrete (SCC) [57]. To counterbalance this effect, the introduction of iron powder with an enlarged bulk density aims to negotiate the possibility of segregation and bleeding by counteracting the ball-bearing effect of other fines in the mix.

Table 3
Segregation and bleeding properties in fresh SCC.

Properties	SCC mix					
	SCCF0	SCCF 5	SCCF 10	SCCF 15	SCCF 20	SCCF 25
Segregation resistance (V Funnel at $T_{5\ min}$)	1.25 s	1.65 s	2.41 s	2.73 s	2.98 s	3.50 s
Bleeding resistance (Visual Stability Index)	VSI 0					VSI I

*VSI 0 indicates a highly stable mix with no evidence of segregation or bleeding and VSI I indicates a stable mix with a slight observation of bleeding and segregation[58].

3.2. Hardened properties

3.2.1. Compressive strength

The mechanical strength at the 7, 14, 28 and 56th day was ascertained by concrete compression test using a universal testing machine. The real-time strength variation is compared and presented in Fig. 7 (a), (b) and (c). Fig. 7(a) shows the compressive strength exhibited by C1 cured samples as a function of the replacement of ferrock in percentage. To understand the relationship of compressive strength with replacement and period of curing polynomial expressions are established and correlated. The experimental results show a good increase in strength, up to 10% substitution of ferrock. The samples SCCF15C1, SCCF20C1, appear to have relatively low strength, and the mix SCCF25C1 shows a poor performance than the control mix. The mix SCCF10C1 showed a peak value of 63.41 MPa and 67 MPa on the 28th and 56th day of water curing (C1). The intruded materials such as metakaolin, fly ash and limestone in ferrock, thus improved the mechanical strength of the concrete by increasing the pozzolanic action with the cement hydrating materials [25,45]. Further, the presence of iron dust in ferrock enhances the crushing value by making the concrete dense and compact [15,37,59]. The strength was higher by11.8%, 21.9% and 20.2% for SCCF5C1, SCCF10C1 and SCCF15C1 at 28 days in the C1 type of curing, and the values were low in SCCF20C1 and SCCF25C1 (-2.3 and −10.7%). This is because of the reduction in the amount of Ca $(OH)_2$ crystallites due to the accelerating hydration effects of the iron fines in concrete [60].

Concerning the compressive strength of C2 samples, they endeavour almost a similar performance as that of C1 type curing. The test results of the samples, immediately after 4 h of CO_2 curing and at 7,14,28 and 56 days were graphically explained in Fig. 7(b). It was found that the application of CO_2 at an early age improves the crystalline form of

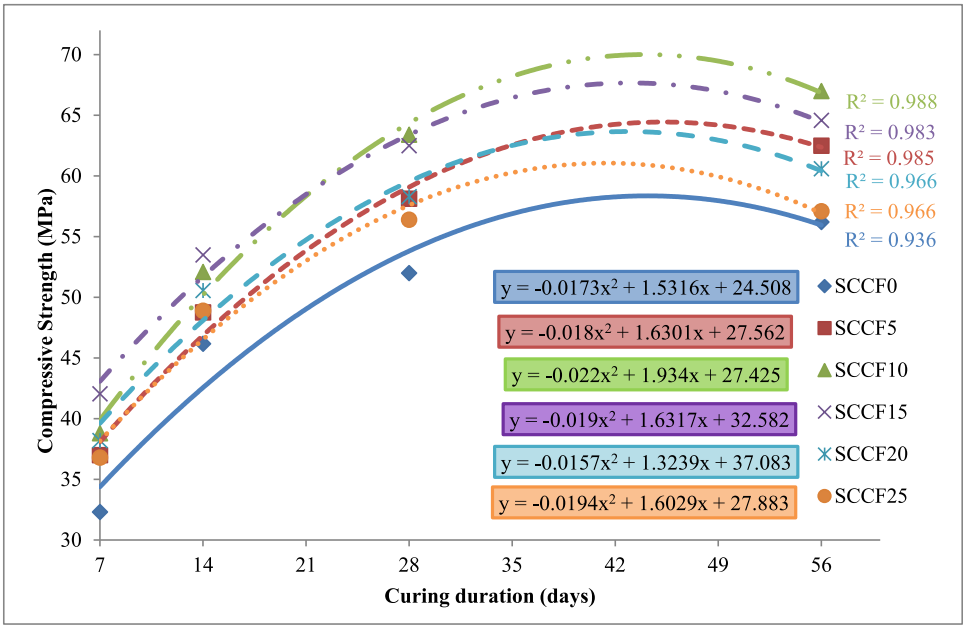

Fig. 7a. Variation of compressive strength with respect to curing duration for C1 curing.

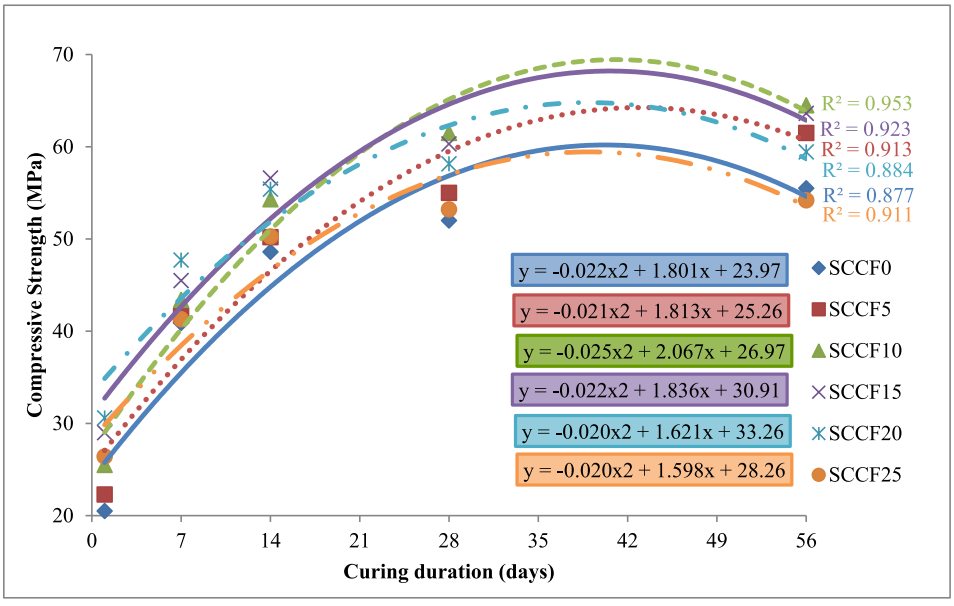

Fig. 7b. Variation of compressive strength with respect to curing duration for C2 curing.

carbonates, thereby acquiring 40% of its strength at an early age. The reactions of calcium silicates (C_3S and C_2S) when they get in contact with CO_2, contribute to earlier strength in CO_2-cured samples. The formation of C-S-H in turn accelerates the carbonation of calcium hydroxide which undergoes a precipitation reaction in the pores of the cement mortar paste resulting in the confinement of pores [61]. This is the primary reason for enhancing the density and durability of carbonated prototypes. Upon addition of ferrock, the absorption and reaction get ameliorated, developing an additional stable ferrous compound ($FeCO_3$) which forms rust, acting like reinforcement for the concrete matrix. This enables improvement in the strength of SCCF10C2 and SCCF15C2 by 25.9% and 24.7% over the control mix (SCCF0C2) at 28 days. Moreover, the pressure maintained in the chamber and the period of exposure to CO_2, probably affect the efficiency of C2 curing [38]. This profound behavior of the concrete under CO_2 curing was rapidly studied in recent times, with an outcome that increased time of exposure to CO_2 accelerates the carbonation reaction [62] ultimately leading to a better construction material comparable to water-bound concrete. It is worth noting that Ca $(OH)_2$ resulting from the hydration process is known to boost up the pozzolanic reactions at later ages. Ultimately, the reduction in $Ca(OH)_2$ during carbonation, cannot activate the silicaceous materials thereby reducing the C-S-H phases in the concrete matrix in later days, impeding the performance of SCC [51]. Even though, the CO_2 curing adopted is sufficient in forming a self-compacting concrete of M40 grade with satisfactory results.

The compressive strength pattern for the C3 type of curing is in line with C1 and C2. But the samples exhibited an extreme strength rate than the others as observed in Fig. 7(c). The samples show a rapid increase in strength for SCCF5C3 and SCCF10C3 followed by a depression at a higher-level incorporation of ferrock at the 28th day. The mixes

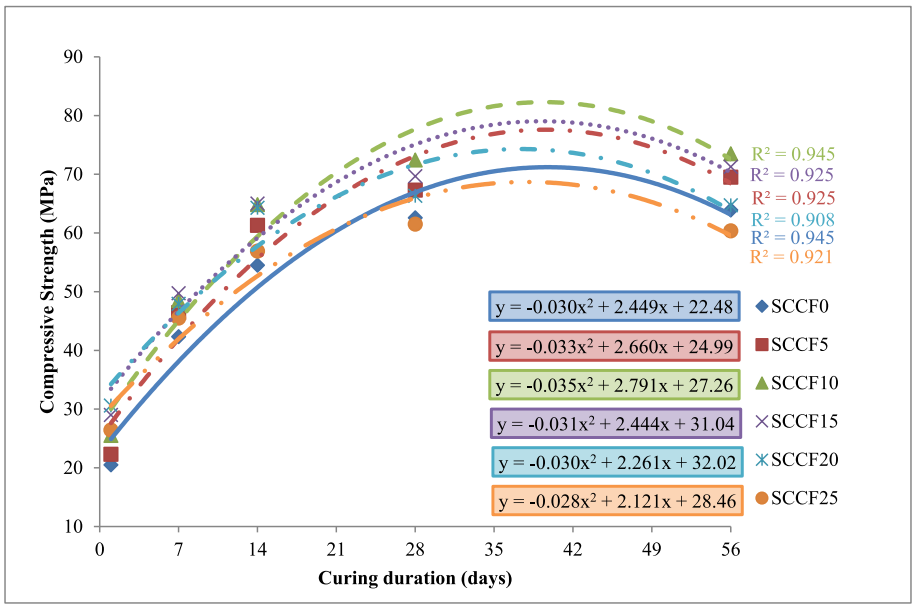

Fig. 7c. Variation of compressive strength with respect to curing duration for C3 curing.

SCCF0C3, SCCF5C3, SCCF10C3 and SCCF15C3 exhibit a high early strength of 42.32, 46.41, 48.5 and 49.73 MPa at 7 days which reaches a peak of 63.9, 69.5, 73.48 and 71.26 MPa at 56 days. This early strength increase was due to the expeditious reaction of iron particles with CO_2 during the first four hours [38]. And during the water curing, the hydration process of C_2S and C_3S expands the quantity of Ca $(OH)_2$ resulting in an intense strength. Since this type of curing facilitates the evolution of both Ca $(OH)_2$ and Fe_2O_3, it greatly enhances the

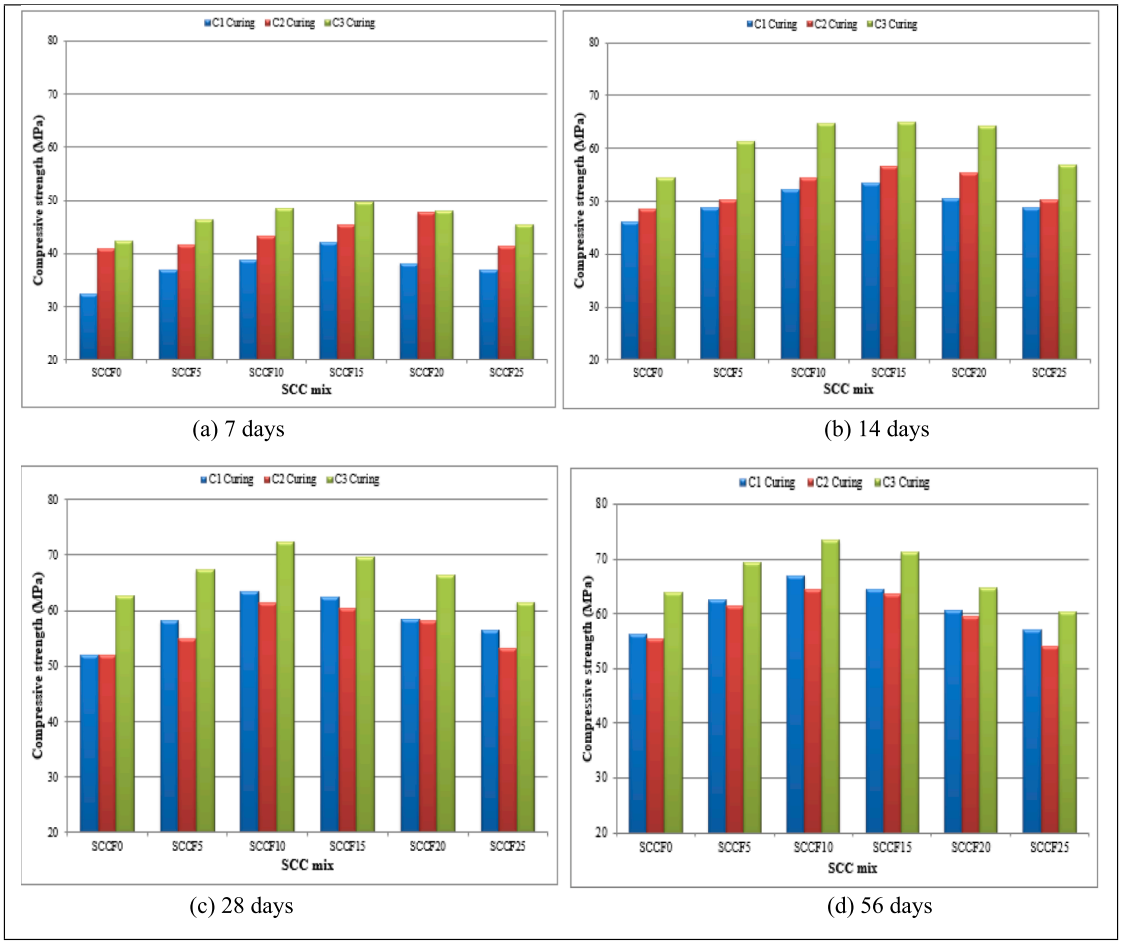

Fig. 8. Comparision of compressive strength at (a) 7 days (b) 14 days (c) 28 days and (d) 56 days.

performance of the concrete. The curve for SCCF15C3 was found to increase gradually for 28 days but exhibited a slight decrease at later ages as seen in Fig. 7(c). This in-efficient performance may be due to the presence of high silica content in ferrock which supports the dilution effect of C_2S and C_3S hindering the pozzolanic reactions occurring at later stages [63].

Fig. 8 provides a comparison of strength development at various curing ages. Notably, while water curing does not allow for immediate strength determination within the first day of setting, CO_2 curing enables testing after a mere 4 h once the samples are removed from the curing tank. Even at 7 days, the SCCF20C2 and SCCF15C3 mixes exhibit nearly double the strength of the control mix SCCF0C1, with observed increases of 47.7% and 53.9% respectively. These results emphasize the superior effectiveness of CO2 curing when compared to conventional water curing, especially during the early stages of curing. Upon reaching 28 and 56 days, the compressive strength of the specimens becomes almost equivalent, for which the SCCF10 mix shows a minimal increase in strength of only 1.5% between 28 and 56 days. Remarkably, at the 56th day, the specimen SCCF10C3, which undergoes both types of curing, demonstrates a 30% higher strength compared to SCCF0 with C1 curing alone, as well as a 32.5% higher strength than C2. These findings highlight the positive impact of incorporating 10% ferrock composite material into the self-compacting concrete.

3.2.2. Tensile strength

The tensile strength of the concrete at 7, 14, and 28 days for C1, C2 and C3 are evaluated by UTM testing. The behavior of the samples under horizontal compression is compared and presented in Table. 4. The effort on the addition of ferrock to SCC, influences the performance of the concrete at a higher level with an increasing rate of strength for up to 10% replacement. A high strength was observed for each addition of ferrock than the control mix (SCCF0) under C1curing. Under C2 curing, the quality of concrete is enhanced by the onsite reaction of iron particles with CO_2, producing a compound of ferric carbonate ($FeCO_3$) as in Eqn. (4) [26], accelerating the disintegration of iron particles which further happens to fill the voids and pores neglecting strength loss [64].

$$Fe + CO_2 + H_2O \rightarrow FeCO_3 + H_2 \quad (4).$$

Upon analyzing the findings, it is observed that the strength percentage varies significantly when ferrock is added, regardless of the duration of testing or the conditions of curing. The control specimens, which underwent C1 and C2 curing, exhibited similar behavior, as evidenced by a minimal 3.3% increase in tensile strength. Under C1 curing, every addition of ferrock exhibited higher strength compared to the control mix (SCCF0) except SCCF20 and SCCF25. While introducing 10% ferrock resulted in a remarkable and consecutive 17%–22% increase in strength across three different curing methods. At all curing ages of 7, 14 and 28 days, maximum resistance was offered by SCCF10, as shown in Table 4. Obviously for the above-said specimen, a maximum tensile strength of 5.23 MPa, 5.31 MPa and 5.57 MPa was observed for C1, C2 and C3 curing at 28 days. These results show the superior behaviour of combined curing C3 over the other cases. The C3 curing exerts a maximum of 30% increase in strength for a 10% addition of ferrock than 28 days water cured control specimen (SCCF0C1). It is also to be noted that after 28 days of C1 and C2 curing, both exhibit almost equal strength development, with a slight variation between 1.5% and 5.7%. Concerning C2 curing, a 20.68% variation was observed between SCCF10 and SCCF0, whereas C1 curing showed a variation of 22.8% for the same. It is worth noting that C2 curing primarily exhibits early-stage strength development with almost 75% of its strength at 7 days but with the incorporation of 10% ferrock, 90% of its strength is achieved early. This early age strength in C2 is due to the dilution and nucleation effect of the ferrock iron powder [59]. The addition of ferrock up to 10%, improves the quality of the mortar paste thereby possessing a good resistance against tension. Works of literature confirm SCC with higher strength at higher paste content [65]. Also, the ferrock imparts additional strength to the SCC by the angular morphology of its iron particles. The iron particles having a rough surface texture form a sturdy interfacial transition zone (ITZ), creating a solid bond between the cement matrix and aggregates thereby improving the strength [66]. Nevertheless, the fine particles in ferrock with its micro filling capacity and pozzolanic activity augment the formation of calcium and aluminium silicates in the silicate and amorphous phases and readily form hydrates empowering concrete. Although, when fly ash and metakaolin were combinedly used in concrete, it may hinder the performance due to the lack of sufficient generation of calcium hydroxide necessary for the formation of C-S-H in the concrete matrix, as a result of which silica particles are left unreacted probably ending in strength reduction [56].

3.2.3. Ultrasonic pulse velocity

UPV yields information on the quality of the concrete in the attribution of pores, voids and packing density of materials. Higher the density of concrete higher will the values in UPV [15]. The determined values of UPV are tabulated in Table. 5. SCC with the inclusion of ferrock in different curing regimes are found satisfactory with values greater than 4000 m/s except for SCCF25C1. As stipulated, the mix with a velocity range of 4500 m/s and above is said to acquire excellent quality whereas 3500 to 4500 m/s are set under good quality concrete specimens [67]. In the present study, good quality of SCC for the control specimen (SCCF0) was observed for C1, C2 and C3 curing. These observations are in turn enhanced with the addition of ferrock at 5, 10 and

Table 5
Ultrasonic pulse velocity of SCC samples at 28 days of different curing conditions in m/s.

SCC mix	Curing environment			Quality of Concrete*
	C1	C2	C3	
SCCF0	4142	4155	4243	Good
SCCF5	4318	4361	4512	Good – Excellent
SCCF10	4676	4687	4922	Excellent
SCCF15	4345	4526	4850	Good – Excellent
SCCF20	4035	4228	4414	Good
SCCF25	3386	4045	4079	Medium – Good

*UPV values ranging between 3500 and 4500 m/s are classified as good quality whereas values above 4500 m/s are represented as excellent [67].

Table 4
Splitting tensile test results (MPa).

SCC mix	Average tensile strength (in days)								
	C1 curing			C2 curing			C3 curing		
	7	14	28	7	14	28	7	14	28
SCCF0	3.28	3.34	4.26	3.15	3.52	4.40	4.16	4.43	4.76
SCCF5	4.37	4.52	4.80	4.46	4.63	4.91	4.55	4.83	5.04
SCCF10	4.77	5.01	5.23	4.80	4.98	5.31	4.91	5.18	5.57
SCCF15	4.01	4.63	5.08	4.22	4.86	5.07	4.47	4.96	5.43
CCF20	3.13	3.41	4.16	3.52	4.02	4.34	3.84	4.18	4.52
SCCF25	3.04	3.21	4.02	3.27	3.76	4.25	3.53	3.88	4.08

15% in all types of curing.

The UPV of SCCF10C1 exhibits a high quality of 4676 m/s of velocity, which reduced the pore structure under morphological study. Similarly, for greater replacement in the C1 category, medium-quality concrete was characterized by weak packing density and increased pores that do not qualify for the standards. Poor mixing of concrete and entrapped air bubbles is yet another reason for the reduction in quality. In CO_2 curing (C2), all mixes were rated as good quality concrete and SCCF5, SCCF10 and SCCF15 excelled compared to other mixes. Similarly, a medium to excellent quality was ensured in the C3 curing for 5 and 10% replacement. Reduction in quality may be subjected to the unreacted compounds present in the mixes, lacking the capacity of filling the voids. The results obtained are quite in compliance with the previously reported results [15,68], for which they used iron slag as a replacement material for fine aggregate and found improvement in the quality of the concrete. The presence of more fine materials thus produces a condensed matrix and compromises the quality of the hardened SCC.

3.3. Bond strength

Any failure of the structurally reinforced members is usually initiated by its bond failure for the assessment of bonding strength becomes crucial in any study. The data as determined by the pull-out test infer the actual interfacial bond behavior between steel rebar and the encompassed concrete materials [69]. The peak load at which the bond between the embedded steel and concrete gets distorted generally represents the bonding strength of the concrete. Fig. 9 illustrates the bonding behavior of various SCC specimens used in the study on the 28th day. The bond strength of the control mix was found 24.3 MPa under C1 curing which gets elevated to 26.34 MPa at combined curing (C3). This infers that the curing conditions play a major role in controlling the strength of the SCC specimens. However, the development of compressive and tensile strength seems closely related to the bonding strength with the addition of ferrock, regardless of the curing conditions. At any rate, the incorporation did not impact negatively up to an optimum percentage of 15% ferrock by weight of the cement. The increase in bond strength for ferrock-incorporated specimens in water curing denoted an enhanced hydration mechanism facilitating pozzolanic reactions at later stages and the filling effect of ultra-fine particles in ferrock at an earlier stage [45]. The improved microstructure of the carbonated specimen (SCCF0C2, SCCF5C2, SCCF10C2, SCCF15C2, SCCF20C2 and SCCF25C2) experiences an enhanced strength than the C1 cured samples by 1.6%, 1.4%, 2.9%, 1%, 0.5% specifically due to the mass increase of carbonation products. For combined curing, the specimens achieved an enhancement of 8.3%, 7.11%, 13.2%, 11.2%, 7% and −0.7% strength variation than the conventional water curing. Thus, improved bond strength was attained at an optimized quantity of 10% substitution of ferrock.

Maximum bond strength was achieved for SCCF10C3 at a range of 29.82 MPa, reporting that impregnating ferrock in cement improves the pull-out resistance by minimizing the propagation of cracks through the dense-compacted SCC-ferrock matrix. The reason is due to the confinement at the substrate-concrete interface, which physically improves the friction between cementitious compounds and complements the mechanical bonding offering resistance to pull-out [44,70]. However, the resistance to pull-out gets reduced beyond an optimum range (0 – 15% by weight of cement), due to the reduction in hydration and carbonation by-products. An increase in the content of ferrock significantly increases the un-hydrated particles resulting in a weak bonding relationship. In this study, SCCF25 acquired lower bond strength than the other mixes, limiting its resistance against pull-out.

3.4. CO_2 uptake

Technically, high pressure of CO_2 sequestration would positively result in accelerating the early-age carbonation reactions in a sample [71]. Also, the efficiency of carbonation is influenced by the duration with which the pressure level is maintained in the chamber. The results obtained by calculating the CO_2 uptake with Eqn.2 are presented in Fig. 10. The figure depicts the CO_2 uptake for an atmospheric condition of 3 bar CO_2 maintained under a high pressure of 350 kPa, for 4 h initially. The carbonated products formed (as mass representation) will present an uptake on the amount of CO_2 absorbed by the specimens. The mass of the samples depends on the reactions of the alite and belite compounds of cement with CO_2, producing abundant quantities of Calcium Silicate Hydrates (C-S-H) and calcium carbonates ($CaCO_3$) [72] as expressed in Eqn. (5), (6) and (7) [38]:

$$3C_3S + (3 - x)\,CO_2 + nH \rightarrow C_xSH_n + (3 - x)\,CaCO_3 \quad (5)$$

$$2\beta - C_2S + (2 - x)\,CO_2 + nH \rightarrow C_xSHn + (2 - x)\,CaCO_3 \quad (6)$$

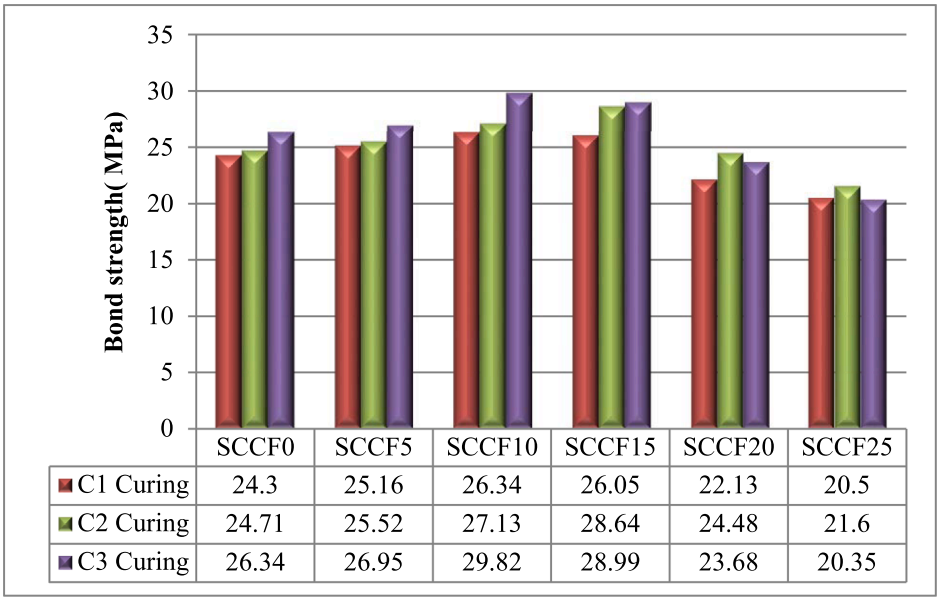

	SCCF0	SCCF5	SCCF10	SCCF15	SCCF20	SCCF25
C1 Curing	24.3	25.16	26.34	26.05	22.13	20.5
C2 Curing	24.71	25.52	27.13	28.64	24.48	21.6
C3 Curing	26.34	26.95	29.82	28.99	23.68	20.35

Fig. 9. Bond strength variation for SCC specimens under miscellaneous curing.

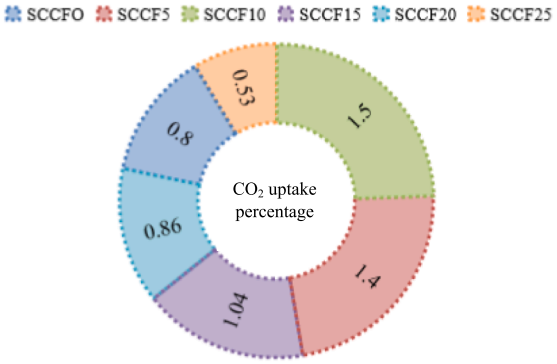

Fig. 10. CO_2 uptake (in percentage) by the SCC specimens for the initial 4 h.

$$Ca(OH)_2 + CO_2 \rightarrow CaCO_3 + H_2O \quad (7)$$

The development and precipitation of these chemical components require CO_2 to be supplied at a continuous rate for a sufficient duration for complete carbonation to take place. Also, the availability of ferrock which is naturally a CO_2-absorbing material speeds up the carbonation reaction resulting in the earlier formation of carbonated by-products. A maximum percentage of intake (1.5%) was observed in SCCF10 samples within 4 h of absorption. However, an increase in the percentage of ferrock was found to lower the properties at its hardened state as discussed in previous sections. SCCF25 samples had a least absorbed percentage of 0.53%. The effectiveness of the 3-bar curing is reasonably the cause for this gradual decrease. Because of the low content of ferrock in SCCF0, SCCF5 and SCCF10 the CO_2 sequestration paves way for deeper penetration of CO_2 gas into the pores of these sample mixtures. As the concentration of ferrock increases, CO_2 tends to react instantly with the ferrock particles at the surface which subsequently reduces the infusion process, thus reducing the rate of reactions deeper inside the samples. This ultimately supports large voids and porosity during hardening, thus causing uncertainty in the properties of strength. Thus, these samples are likely to be carbonized at the surface and found to have no deeper penetration depth. In addition, the duration of carbonation act as a major factor in determining the strength of the concrete. On increasing the carbon uptake duration, the CO_2 penetrates deeper into the core establishing a reduced mass loss between the surface and core [9]. For 5,10 and 15% ferrock infusion, increasing the time of curing will ultimately lead to an increase in properties. When iron dust in Ferrock is exposed to carbon dioxide, it transforms into a solid material that is five times stronger than regular concrete and has a higher CO_2 absorption capacity [26]. However, when combined with cement, its effectiveness is underestimated.

3.5. Cement use efficiency

The sensational achievement of the incorporation of any industrial waste depends on its performance of sustainability. The sustainability of the SCC-ferrock combination is the reduction in procurement of CO_2-emitting material for a good cause. Fig. 11 shows the cement use efficiency indexes obtained for 28 days of cured samples under different curing domains. The indexes obtained for ferrock -SCCs were subsequently lower than the control SCC mixes. In practical applications of water curing, the cement use efficiency was deduced from 10.6 kgm^{-3} MPa^{-1} to 7.48 kgm^{-3} MPa. It is because of the contribution of nucleation sites by the limestone powder, improved silica content from fly ash and cohesive nature of metakaolin imparted in the ferrock [9]. The results correlate to the study of Pelisser et al [73], which marked an index of 7.8 kgm^{-3} Mpa^{-1}. Long et al [48] tried to develop a low binder SCC and acquired similar sustainability cement indices.

On CO_2 curing, cement use efficiency was reduced to 7.42 kgm^{-3} MPa^{-1} from an extremity of 10.9 kgm^{-3} MPa^{-1}. A peak reduction was observed for the third type of curing which depreciates the index from 9.26 to 6.19 kgm^{-3} MPa^{-1}, which was found most beneficial. On interpretation of the results, ferrock replaced with cement by 10%, possesses a compromising strength with a significant cement use efficiency index. The study was found to potentially enhances the

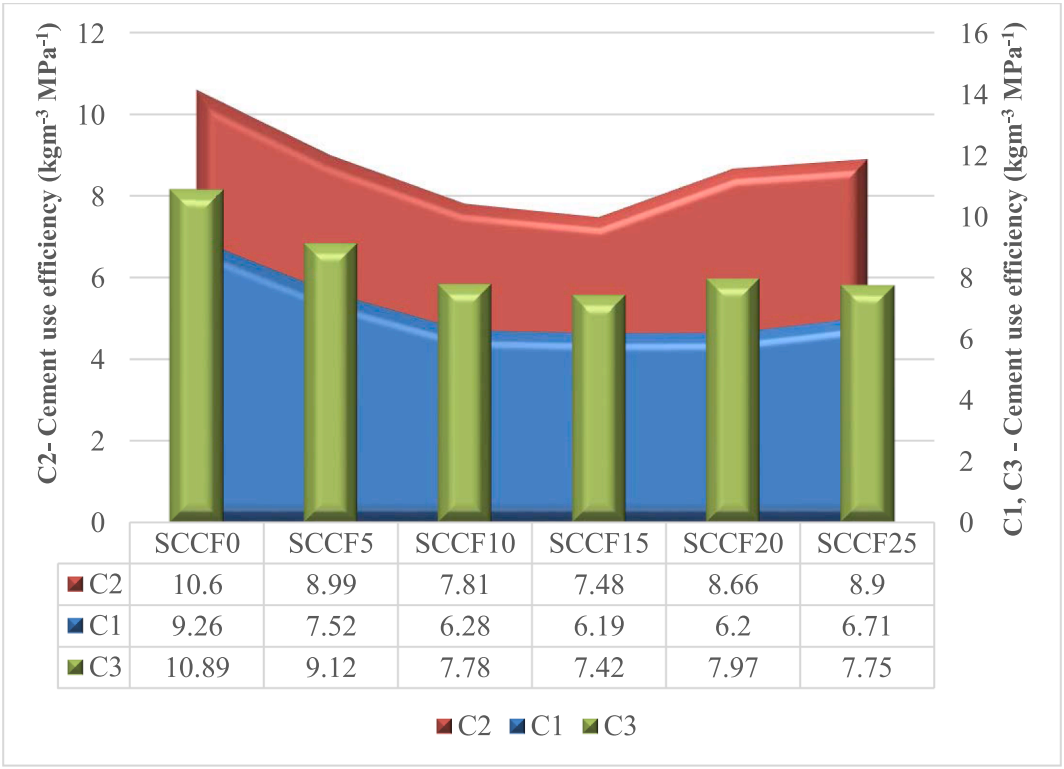

Fig. 11. Cement use efficiency of SCC specimens cured at C1, C2 and C3 environment.

sustainability behavior of ferrock on self-compacting concrete by creditably decreasing the cement content in concrete.

3.6. Microstructural characterization

3.6.1. X-ray diffraction (XRD)

The different patterns of the mineralogical composition obtained for the samples cured under different conditions of curing are visualized in Fig. 12. The formation of hydrated and carbonated by-products with their peak composition are analyzed and compared. Six samples were eventually analyzed, of which three were control specimens under the C1, C2 and C3 type of curing, whereas the other three were 10% ferrock-incorporated SCC specimens. Fe, Mg, Si, Al bearing reactive compounds were observed in respective samples along with the commonly visible peaks of $Ca(OH)_2$ (otherwise called portlandite), calcium silicate hydrate (C-S-H), calcium alumina silicate hydrate (C-A-S-H) and quartz form of silica (SiO_2). Quartz was observed commonly in all the specimens at major peaks. Water-cured samples SCCF0C1 in Fig. 12(a) show peaks of quartz, portlandite, calcium silicate hydrates, CASH and minor quantities of calcite crystal and ettringite formation. Whereas, ferrock incorporated SCCF10C1 possess a traceable amount of hedenbergite ($CaFe_2Si_2O_6$), magnesium ferrite ($MgFe_2O_4$), and calcium - magnesium alumina silicate (CMAS) phases due to the prominent reaction of C_2S and C_3S with supplementary cementitious add-on material (ferrock).

Specimens cured at C2, showed calcite ($CaCO_3$) as the predominant mineral of carbonation, followed by metastable phases of $CaCO_3$ rarely available as aragonite as indicated in Fig. 12(b). The effectiveness of the curing hours may influence the conversion of these metastable by-products to a stable calcite form. However, the early age strength of SCC is contributed by the formation of the above-mentioned *meta*-stable compounds. The carbonation reactions also support the formation of CSH, CASH, magnesite ($MgCO_3$) and quartz which facilitates the development of a strong interfacial transition zone (ITZ) and a dense matrix structure. Ferrock-based SCC when undergoing carbonation tends to produce siderite ($FeCO_3$), a solid carbonate of iron particles, which often indicates the rusting of iron artefacts. Herein the study, this mineral composition tends to improve the microstructure by filling the voids left even after the formation of CSH, thereby improving the porous nature of the SCC Matrix [60].

Distinct peaks of cumulative mineral phases of C1 and C2 were observed for C3 samples as represented in Fig. 12(c). 4 h of carbonation followed by hydration consequently reduces the intensity of peaks for calcium phases (calcite, Portlandite & Dolomite). Apart from C2 curing, these samples show a balanced formation of Calcite and Portlandite formation with abundant C-S-H. Since calcite and aragonite are polymorphs of calcium carbonate, this type of curing allows the formation of stable $CaCO_3$, eliminating aragonite and resulting in high strength and performance. In turn, the availability of Fe_2O_3 in ferrock emphasizes the formation of ettringites ($Ca_6Al_2(SO_4)_3\ OH_{12}\ 26H_2O$), in reaction with calcium hydroxides [74]. The mineralogical phases of iron were found dominant under all reactions because of the inert nature of other materials (fly ash, metakaolin and limestone) in the mix. Further, C-S-H and C-A-S-H phases were abundant in all the samples due to the excess

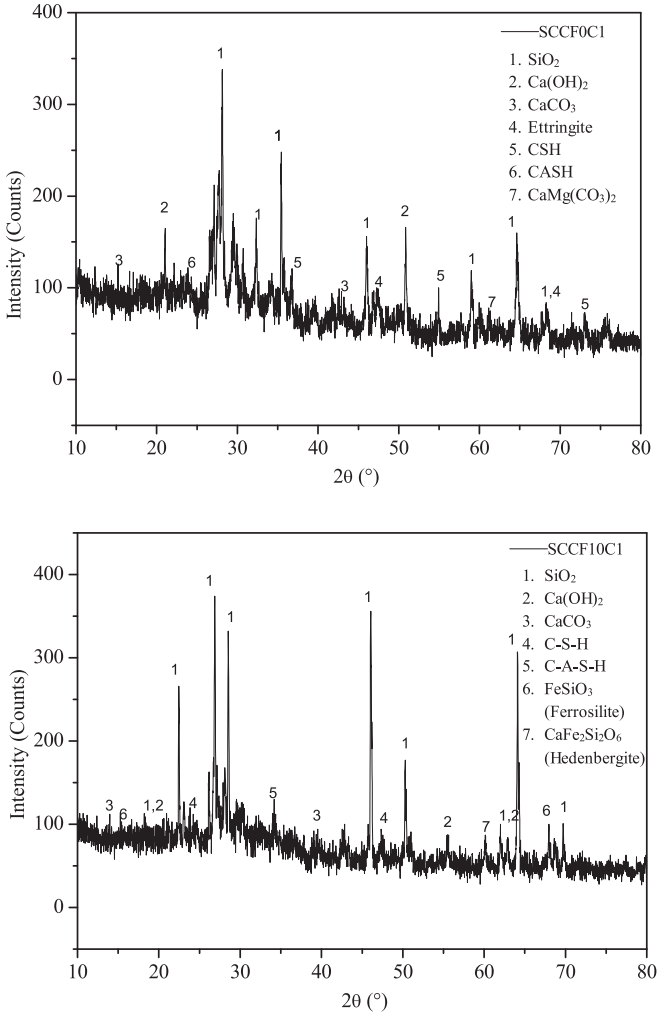

Fig. 12a. XRD for specimens SCCF0 and SCCF10 under C1 curing.

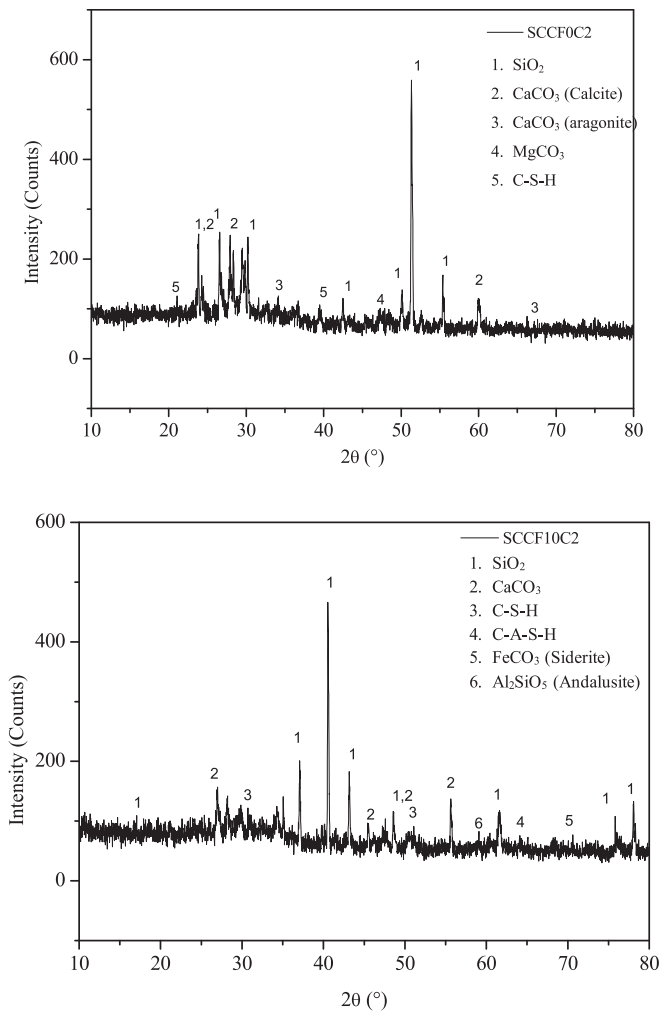

Fig. 12b. XRD for specimens SCCF0 and SCCF10 under C2 curing.

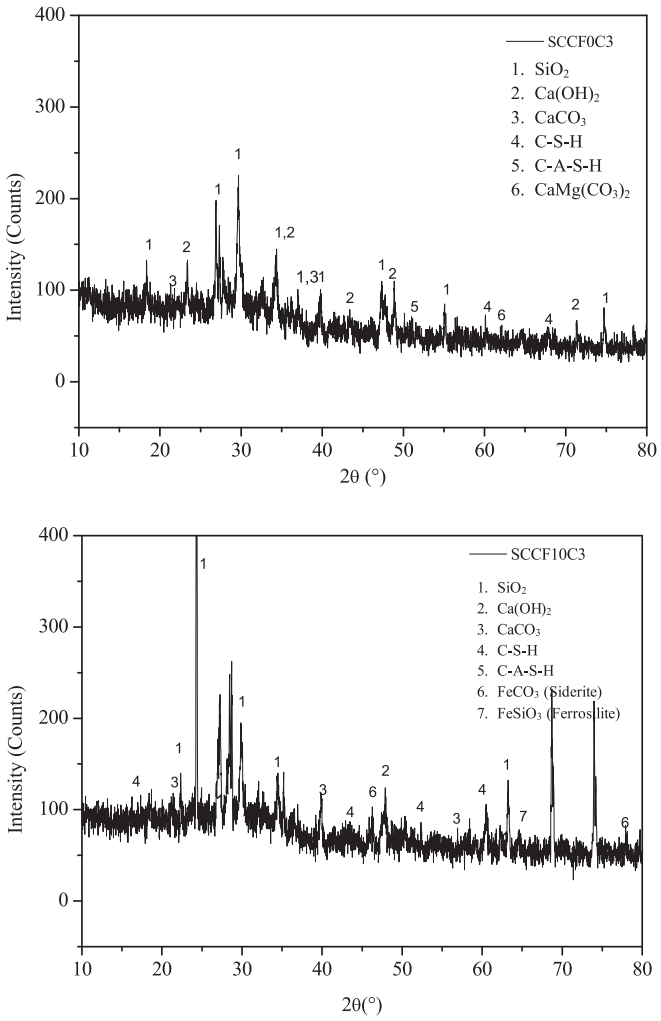

Fig. 12c. XRD for specimens SCCF0 and SCCF10 under C3 curing.

silicates and aluminates, which impart additional strength to the SCC [63].

3.6.2. *Scanning electron microscope (SEM)*

The microstructural characterization forms the deciding factors for the strength and rheological properties of the concrete and is yet to be studied in its deeper concept. The micrographs obtained from SEM analysis for the typical SCC specimens were presented in Fig. 13. The figure depicts the presence of hydrated phases of calcium in portlandite, calcite and C-S-H. Fig. 13(a) representing the specimen SCCF0C1 pictures the absence of dense C-S-H gel, but with ample availability of Ca $(OH)_2$, ettringite and $CaCO_3$. The bond between the particles was quite undesirable, as the propagation of hairline cracks was visible through the concrete matrix and pores were widely distributed. For the mix made with ferrock (SCCF10C1), the visualization looks similar but with a slight improvement in the dense C-S-H gel formation. Fig. 12 (a) images the presence of ettringite and calcium iron silicates (Hedenbergite) with a substantial reduction in pores and voids providing better performance than SCCF0C1.

The $CaCO_3$ is formed as the immediate by-product of carbonation, representing a stable solid product contributing strength in SCC. Fig. 13 (b), specifies the availability of denser C-S-H gel than C1 samples with amorphous phases of calcite and aragonite. However, improving the duration of CO_2 curing could sufficiently enhance the homogeneity of the carbonated specimens. For SCCF10C2, $CaCO_3$ and calcium silicates are formed in addition to iron carbonate due to the ample availability of Ca, Si and Al ions provided by ferrock as cementing materials.

The SEM images for SCCF0C3 show reduced content of ettringites, portlandite and calcite with uneven calcium silicate hydrate (CSH) layers formed from the carbonation and continuous hydration. But the ferrock-infused SCC samples (SCCF10C3) under C3 curing provide a uniform dense C-S-H formation with prominent iron carbonates which becomes responsible for its mechanical strength and voids reduction. The existence of an interfacial transition zone between the cement paste and aggregates is also clearly seen in Fig. 13(c). Concatenating the SEM micrographs with XRD inference and mechanical behavior, the progressive growth in strength is primarily dependent on the development of the C-S-H gel structure within the matrix [2]. The refinement in pore structure is due presence of micro-fillers in ferrock which significantly fills the gap between cement particles and supports pozzolanic reactions at later stages. The SEM microstructure is expected to be at its best at 90 and 365 days since pozzolanic reactions found its way of slow progression.

4. Conclusion

In summary, the experimental investigation in this study aimed to identify the optimal replacement of ferrock in SCC while maintaining concrete strength and to assess the feasibility of developing ferrock-based SCC without CO_2 curing. The results showed that SCC mixes

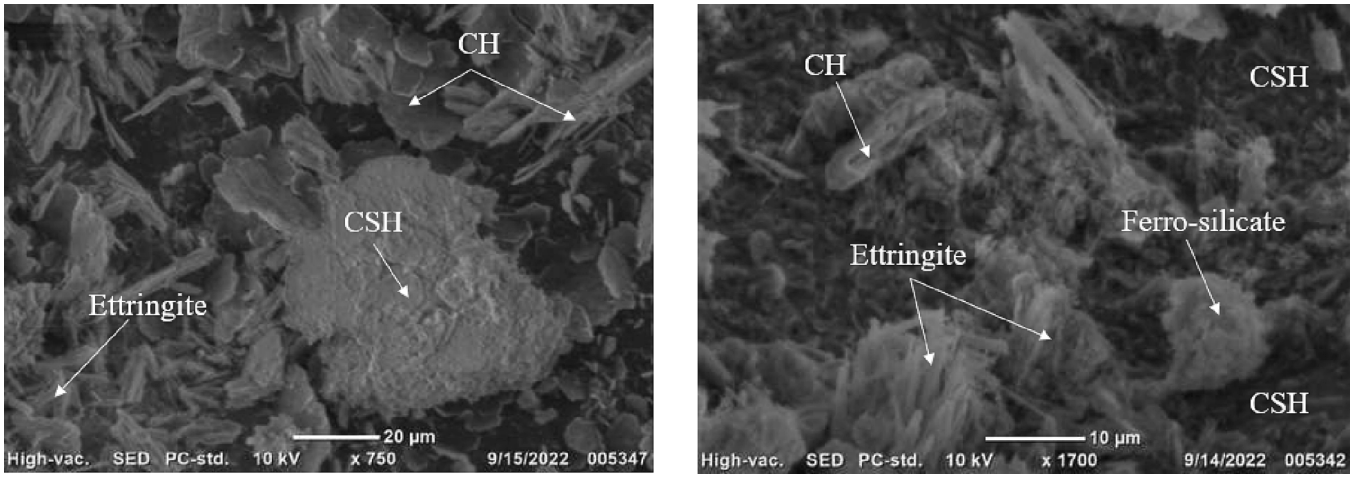

Fig. 13a. Micro-photographs of specimens SCCF0 and SCCF10 under C1 curing (Ettringite represents needle-like structures, CH– Calcium hydroxide, FS- Ferro-silicate, CSH- Calcium silicate hydrate).

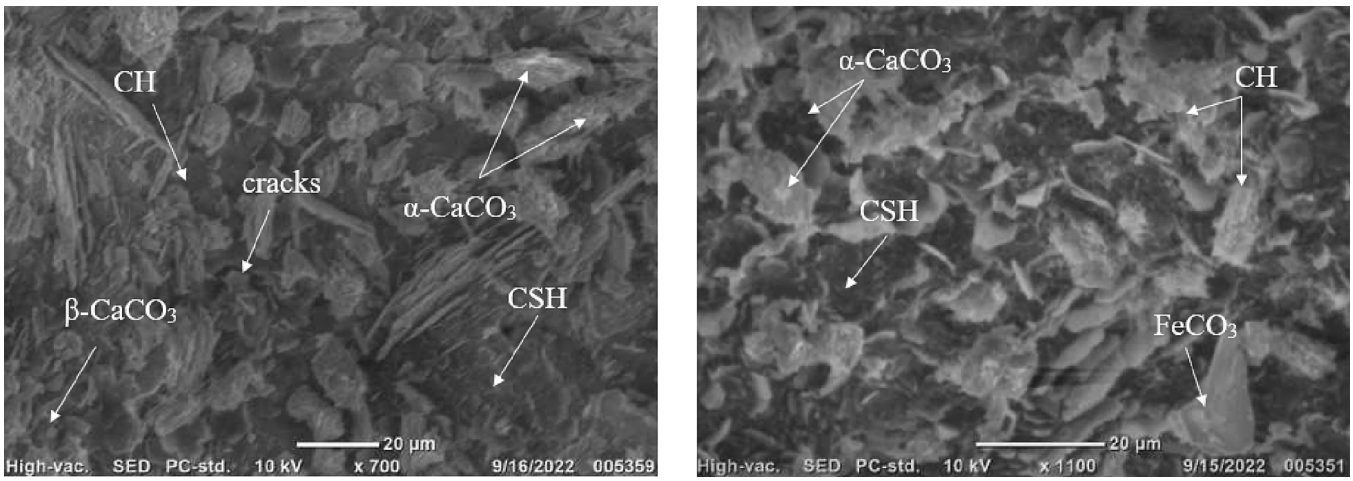

Fig. 13b. Micro-photographs of specimens SCCF0 and SCCF10 under C2 curing (CH represents Calcium hydroxide, α-$CaCO_3$- Calcite, β-$CaCO_3$- Aragonite, $FeCO_3$- Siderite, CSH- Calcium silicate hydrate.

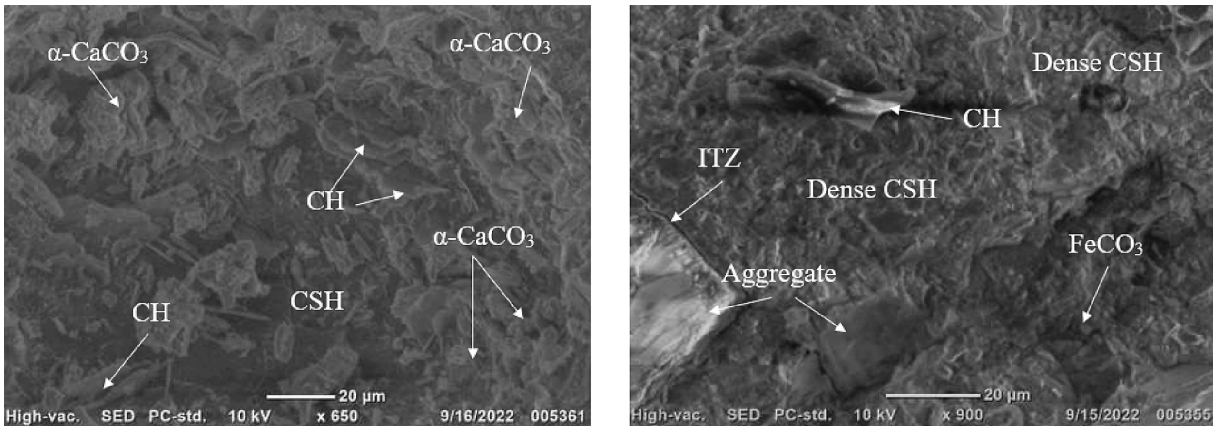

Fig. 13c. Micro-photographs of specimens SCCF0 and SCCF10 under C3 curing (CH represents Calcium hydroxide, α-$CaCO_3$- Calcite, β-$CaCO_3$ fully consumed, $FeCO_3$- Siderite, CSH- Calcium silicate hydrate, ITZ- Interfacial transition zone).

containing up to 15% ferrock exhibited satisfactory properties in terms of viscosity and flowability, and the addition of 10% ferrock to SCC resulted in excellent hardened characteristics at 7, 14, 28, and 56 days. All curing methods yielded reliable performance up to 15% of ferrock. The tensile performance of SCC mixes improved by 20% with 10% ferrock substitution in all curing regimes, and the ultrasonic pulse velocity test indicated good and excellent concrete quality for up to 15% replacement of ferrock.

Moreover, the use of ferrock in SCC enhanced the material's efficiency in CO_2 uptake and cement consumption, yielding positive environmental benefits. The experimental results suggest an optimum of 10% ferrock for developing sustainable concrete. Differences in strength due to variations in curing conditions were negotiable, indicating the practical application of conventional water curing instead of CO_2 curing. This initiative could reduce industrial waste dumping on fertile lands and provide practical applications for strengthening reinforcements in concrete.

However, further studies are required to investigate the flexural properties and crack patterns of structural elements developed using the optimized ferrock percentage in SCC. Long-term durability behavior on water absorption, sulphate resistance, acid attack, stress–strain behavior, and shrinkage assessment need further investigation. Additionally, studies on CO_2 absorption and emission characteristics could pave the way for sustainability in adopting this carbon-negative material.

In conclusion, the present study demonstrates the potential of ferrock in SCC as a sustainable and environmentally friendly construction material. The findings of this research could be beneficial for engineers, architects, and construction professionals in the development of sustainable construction practices, while reducing the negative impact on the environment.

Author Contributions

J. Jeffy Pravitha, R. Ninija Merina and N. Subash contributed to the implementation of the research and writing of the manuscript. All authors have written, read and agreed to the published version of the manuscript.

Declaration of Competing Interest

The authors declare that they have no known competing financial interests or personal relationships that could have appeared to influence the work reported in this paper.

Data availability

Data will be made available on request.

Acknowledgements

The authors gratefully acknowledge the publication support given by the Department of Civil Engineering, University College of Engineering, Nagercoil.

References

[1] A. Karimipour, M. Ghalehnovi, J. de Brito, M. Attari, The effect of polypropylene fibres on the compressive strength, impact and heat resistance of self-compacting concrete, Structures. 25 (2020) 72–87, https://doi.org/10.1016/j.istruc.2020.02.022.
[2] B.C. Xavier, E. Verzegnassi, A.D. Bortolozo, S.M. Alves, R.C. Cecche Lintz, L. Andreia Gachet, W.R. Osório, Fresh and Hardened States of Distinctive Self-Compacting Concrete with Marble- and Phyllite-Powder Aggregate Contents, J. Mater. Civ. Eng. 32 (2020), https://doi.org/10.1061/(asce)mt.1943-5533.0003103.
[3] H. Okamura, M. Ouchi, Self-Compacting Concrete, ACT 1 (1) (2003) 5–15.
[4] M.R. Md Zain, C.L. Oh, S.W. Lee, Investigations on rheological and mechanical properties of self-compacting concrete (SCC) containing 0.6 μm eggshell as partial replacement of cement, Constr. Build. Mater. 303 (2021), https://doi.org/10.1016/j.conbuildmat.2021.124539.
[5] V. Jayanthi, S. Avudaiappan, M. Amran, K.P. Arunachalam, D.N. Qader, M. C. Delgado, E.I. Saavedra Flores, R.S.M. Rashid, Innovative use of micronized biomass silica-GGBS as agro-industrial by-products for the production of a sustainable high-strength geopolymer concrete, Case Stud, Constr. Mater. 18 (2023) e01782.
[6] N. Subash, S. Avudaiappan, S. Adish Kumar, M. Amran, N. Vatin, R. Fediuk, R. Aepuru, Experimental investigation on geopolymer concrete with various sustainable mineral ashes, Materials (Basel). 14 (24) (2021) 7596.
[7] Unep, Global Status Report for Buildings and Construction, Glob. Status Rep. 2020 (2020) 20–24. http://www.un.org/Depts/.
[8] A. Lanuza, A.T. Achaiah, J. Bello, T. Donovan, Ferrock: a Life Cycle Comparison To Ordinary Portland Cement, (2017) 1–24. http://ironkast.com/wp-content/uploads/2017/11/USC-Ferrock-Final-Paper-4.24.17.pdf.
[9] S. Das, B. Souliman, D. Stone, N. Neithalath, Synthesis and properties of a novel structural binder utilizing the chemistry of iron carbonation, ACS Appl. Mater. Interfaces. 6 (2014) 8295–8304, https://doi.org/10.1021/am5011145.
[10] G. of I. Ministry of Steel, Ministry of Steel - Government of India, Annu. Rep. 2020-21. (2020).
[11] G. of I. Ministry of Steel, Ministry of Steel - Government of India, Annu. Rep. 2019-20. (2019).
[12] K. Katam, M.P. Gundupalli, D. Bhattacharyya, Urbanization Challenges in Emerging Economies, in: Urban. Challenges Emerg. Econ. Energy Water Infrastructure; Transp. Infrastructure; Plan. Financ. - Sel. Pap. from ASCE India Conf. 2017, 2017: pp. 278–287.
[13] J. Kargin, L.D.L.S. Valladares, L.E. Borja-Castro, J. Xize, D.G. Mukhambetov, Y. V. Konyukhov, N.O. Moreno, A.G.B. Dominguez, C.H.W. Barnes, Characterization of iron oxide waste scales obtained by rolling mill steel industry, Hyperfine Interact. 243 (2022), https://doi.org/10.1007/s10751-022-01800-7.
[14] A. Lorenzi, D. Rastelli, A. Biavati, M. Poncini, I. Alfieri, F. Albertini, E. Gombia, L. Romaniello, A. Montenero, Immobilization of iron rich steel industry waste and products characterization, J. Environ. Chem. Eng. 3 (2015) 196–201, https://doi.org/10.1016/j.jece.2014.11.024.
[15] G. Singh, R. Siddique, Strength properties and micro-structural analysis of self-compacting concrete made with iron slag as partial replacement of fine aggregates, Constr. Build. Mater. 127 (2016) 144–152, https://doi.org/10.1016/j.conbuildmat.2016.09.154.
[16] G. Singh, R. Siddique, Effect of iron slag as partial replacement of fine aggregates on the durability characteristics of self-compacting concrete, Constr. Build. Mater. 128 (2016) 88–95, https://doi.org/10.1016/j.conbuildmat.2016.10.074.
[17] S. Sarsam, S. Issa Sarsam, Influence of Nano Materials Addition as Partial Replacement of Cement in the Properties of Concrete Pavement Warm Mix Asphalt Concrete View project NDT FOR EVALUATING ASPHALT CONCRETE View project Influence of Nano Materials Addition as Partial Replacement of Cement in the Properties of Concrete Pavement, 2016. http://www.aiscience.org/journal/jnnhttp://creativecommons.org/licenses/by-nc/4.0/.
[18] X. Huang, R. Ranade, V.C. Li, Feasibility Study of Developing Green ECC Using Iron Ore Tailings Powder as Cement Replacement, J. Mater. Civ. Eng. 25 (2013) 923–931, https://doi.org/10.1061/(asce)mt.1943-5533.0000674.
[19] P. Nanthagopalan, M. Santhanam, Fresh and hardened properties of self-compacting concrete produced with manufactured sand, Cem. Concr. Compos. 33 (2011) 353–358, https://doi.org/10.1016/j.cemconcomp.2010.11.005.
[20] M. Mehrinejad Khotbehsara, E. Mohseni, T. Ozbakkaloglu, M.M. Ranjbar, Retracted: Durability Characteristics of Self-Compacting Concrete Incorporating Pumice and Metakaolin, J. Mater. Civ. Eng. 29 (2017), https://doi.org/10.1061/(asce)mt.1943-5533.0002068.
[21] S.T. Aly, A.S. El-Dieb, M.R. Taha, Effect of High-Volume Ceramic Waste Powder as Partial Cement Replacement on Fresh and Compressive Strength of Self-Compacting Concrete, J. Mater. Civ. Eng. 31 (2019), https://doi.org/10.1061/(asce)mt.1943-5533.0002588.
[22] O.R. Kavitha, V.M. Shanthi, G. Prince Arulraj, P. Sivakumar, Fresh, micro- and macrolevel studies of metakaolin blended self-compacting concrete, Appl. Clay Sci. 114 (2015) 370–374, https://doi.org/10.1016/j.clay.2015.06.024.
[23] N. Subash, S. Adish Kumar, A simplified geopolymer concrete mix design considering five mineral admixtures, Eur. J. Environ. Civ. Eng. 26 (15) (2022) 7572–7585.
[24] A. Singh, S. Arora, V. Sharma, B. Bhardwaj, Workability Retention and Strength Development of Self-Compacting Recycled Aggregate Concrete Using Ultrafine Recycled Powders and Silica Fume, J. Hazardous, Toxic, Radioact. Waste. 23 (2019), https://doi.org/10.1061/(asce)hz.2153-5515.0000456.
[25] R. Prakash, S.N. Raman, N. Divyah, C. Subramanian, C. Vijayaprabha, S. Praveenkumar, Fresh and mechanical characteristics of roselle fibre reinforced self-compacting concrete incorporating fly ash and metakaolin, Constr. Build. Mater. 290 (2021) 123209.
[26] D.S. Vijayan, Dineshkumar, S. Arvindan, T. Shreelakshmi Janarthanan, Evaluation of ferrock: A greener substitute to cement, Materials Today: Proceedings 22 (2020) 781–787.
[27] IS 12269: 2013, IS 12269 : 2013- 53 grade ordinary Portland cement — SPECIFICATION, 1967.
[28] BIS:3812-1981, Specification for fly ash for use as pozzolana and admixture, Bur. Indian Stand. New Delhi, India. (1992).
[29] M.A. Legodi, D. de Waal, The preparation of magnetite, goethite, hematite and maghemite of pigment quality from mill scale iron waste, Dye. Pigment. 74 (2007) 161–168, https://doi.org/10.1016/j.dyepig.2006.01.038.
[30] J. Dunkley, M. Martín, F. López, M. Rabanal, J. Torralba, Production of Sponge Iron Powder by Reduction of a By-product of the Steelmaking Industry, n.d.
[31] L. Rahman, S. Bhattacharjee, S. Islam, F. Zahan, B. Biswas, N. Sharmin, A study on the preparation and characterization of maghemite (γ-Fe2O3) particles from iron-containing waste materials, J. Asian Ceram. Soc. 8 (2020) 1083–1094, https://doi.org/10.1080/21870764.2020.1812838.
[32] Indian Stand. 383 (1970) 1–24.
[33] IS:2386 (Part I), Method of test for aggregate for concrete (Particle size and shape), 1963.
[34] IS 9103, Specification for Concrete Admixtures, Bur. Indian Stand. Delhi. (1999) 1–22.
[35] A.I. Al-Negheimish, G. Fares, A.M. Alhozaimy, M. Iqbal Khan, Visual-Based Evaluation Method for Optimizing the Dosage of PCE-Based Superplasticizer for SCC Paste and Concrete Mixtures, J. Mater. Civ. Eng. 30 (2018), https://doi.org/10.1061/(asce)mt.1943-5533.0002374.
[36] EFNARC, The European Guidelines for Self-Compacting Concrete: Specification, Production and Use, 2005. www.efnarc.org.
[37] M.A. Largeau, R. Mutuku, J. Thuo, Effect of Iron Powder (Fe₂O₃) on Strength, Workability, and Porosity of the Binary Blended Concrete, Open, J. Civ. Eng. 08 (2018) 411–425, https://doi.org/10.4236/ojce.2018.84029.
[38] S.H. Han, Y. Jun, T.Y. Shin, J.H. Kim, CO_2 curing efficiency for cement paste and mortars produced by a low water-to-cement ratio, Materials (Basel). 13 (17) (2020) 3883.
[39] F. Concrete, IS-1199-2018 Fresh Concrete, in: 2018.
[40] IS 516, Method of Tests for Strength of Concrete, Bur. Indian Stand. (1959) 1–30.
[41] IS 5816-1999, Indian standard Splitting tensile strength of concrete- method of test, Bur. Indian Stand. (1999) 1–14.
[42] American Society for Testing and Material, ASTM C 597-02, Standard test Method For Pulse Velocity Through Concrete, 2003.
[43] RILEM TC, RC 6 Bond test for reinforcement steel. 2. Pull-out test, in: RILEM Recomm. Test. Use Constr. Mater., 1994. https://doi.org/10.1617/2351580117.081.
[44] M. Gesoğlu, E. Güneyisi, R. Alzeebaree, K. Mermerdaş, Effect of silica fume and steel fiber on the mechanical properties of the concretes produced with cold bonded fly ash aggregates, Constr. Build. Mater. 40 (2013) 982–990, https://doi.org/10.1016/j.conbuildmat.2012.11.074.
[45] H.-A. Nguyen, T.-P. Chang, J.-Y. Shih, Engineering Properties and Bonding Behavior of Self-Compacting Concrete Made with No-Cement Binder, J. Mater. Civ. Eng. 30 (2018), https://doi.org/10.1061/(asce)mt.1943-5533.0002136.
[46] M. Mahoutian, Z. Ghouleh, Y. Shao, Carbon dioxide activated ladle slag binder, Constr. Build. Mater. 66 (2014) 214–221, https://doi.org/10.1016/j.conbuildmat.2014.05.063.
[47] B.L. Damineli, F.M. Kemeid, P.S. Aguiar, V.M. John, Measuring the eco-efficiency of cement use, Cem. Concr. Compos. 32 (2010) 555–562, https://doi.org/10.1016/j.cemconcomp.2010.07.009.
[48] W.J. Long, Y. Gu, J. Liao, F. Xing, Sustainable design and ecological evaluation of low binder self-compacting concrete, J. Clean. Prod. 167 (2017) 317–325, https://doi.org/10.1016/j.jclepro.2017.08.192.
[49] A. Joshaghani, M. Balapour, M. Mashhadian, T. Ozbakkaloglu, Effects of nano-TiO2, nano-Al2O3, and nano-Fe2O3 on rheology, mechanical and durability properties of self-consolidating concrete (SCC): An experimental study, Constr. Build. Mater. 245 (2020) 118444.
[50] M.A.S. Anjos, A. Camões, P. Campos, G.A. Azeredo, R.L.S. Ferreira, Effect of high volume fly ash and metakaolin with and without hydrated lime on the properties of self-compacting concrete, J. Build. Eng. 27 (2020) 100985.
[51] L. Zhou, Y.u. Zheng, Y. Yu, G. Song, L. Huo, Y. Guo, Experimental study of mechanical and fresh properties of HVFA-SCC with and without PP fibers, Constr. Build. Mater. 267 (2021) 121010.
[52] D. Wang, C. Shi, N. Farzadnia, Z. Shi, H. Jia, A review on effects of limestone powder on the properties of concrete, Constr. Build. Mater. 192 (2018) 153–166, https://doi.org/10.1016/j.conbuildmat.2018.10.119.
[53] P.R. da Silva, J. de Brito, Durability performance of self-compacting concrete (SCC) with binary and ternary mixes of fly ash and limestone filler, Mater. Struct. Constr. 49 (2016) 2749–2766, https://doi.org/10.1617/s11527-015-0683-6.

[54] N. Diamantonis, I. Marinos, M.S. Katsiotis, A. Sakellariou, A. Papathanasiou, V. Kaloidas, M. Katsioti, Investigations about the influence of fine additives on the viscosity of cement paste for self-compacting concrete, Constr. Build. Mater. 24 (2010) 1518–1522, https://doi.org/10.1016/j.conbuildmat.2010.02.005.
[55] A.S. Gill, R. Siddique, Strength and micro-structural properties of self-compacting concrete containing metakaolin and rice husk ash, Constr. Build. Mater. 157 (2017) 51–64, https://doi.org/10.1016/j.conbuildmat.2017.09.088.
[56] B. Felekoğlu, S. Türkel, B. Baradan, Effect of water/cement ratio on the fresh and hardened properties of self-compacting concrete, Build. Environ. 42 (2007) 1795–1802, https://doi.org/10.1016/j.buildenv.2006.01.012.
[57] P. Zhang, Q.F. Li, Combined effect of polypropylene fiber and silica fume on workability and carbonation resistance of concrete composite containing fly ash, Proc. Inst. Mech. Eng. Part L J. Mater. Des. Appl. 227 (2013) 250–258, https://doi.org/10.1177/1464420712458198.
[58] Astm c1611,, Standard Test Method for Slump Flow of Self-Consolidating Concrete, ASTM Int. i (2018) 6.
[59] F. Han, Y.u. Zhou, Z. Zhang, Effect of gypsum on the properties of composite binder containing high-volume slag and iron tailing powder, Constr. Build. Mater. 252 (2020) 119023.
[60] J.A. Abdalla, B.S. Thomas, R.A. Hawileh, J. Yang, B.B. Jindal, E. Ariyachandra, Influence of nano-TiO2, nano-Fe2O3, nanoclay and nano-CaCO3 on the properties of cement/geopolymer concrete, Clean. Mater. 4 (2022) 100061.
[61] B.A. Tayeh, D.M. Al Saffar, Utilization of Waste Iron Powder as Fine Aggregate in Cement Mortar, 2018.
[62] S.O. Omale, T.S.Y. Choong, L.C. Abdullah, S.I. Siajam, M.W. Yip, Utilization of Malaysia EAF slags for effective application in direct aqueous sequestration of carbon dioxide under ambient temperature, Heliyon. 5 (10) (2019) e02602.
[63] R. Choudhary, R. Gupta, R. Nagar, Impact on fresh, mechanical, and microstructural properties of high strength self-compacting concrete by marble cutting slurry waste, fly ash, and silica fume, Constr. Build. Mater. 239 (2020) 117888.
[64] J.J. Kim, Y.S. Heo, T. Noguchi, Effect of iron powder on inhibition of carbonation process in cementitious materials, ISIJ Int. 55 (2015) 1522–1530, https://doi.org/10.2355/isijinternational.55.1522.
[65] G. Rodriguez de Sensale, I. Rodriguez Viacava, A. Aguado, Simple and Rational Methodology for the Formulation of Self-Compacting Concrete Mixes, J. Mater. Civ. Eng. 28 (2016), https://doi.org/10.1061/(asce)mt.1943-5533.0001375.
[66] M.J. Miah, M.K. Ali, S.C. Paul, A. John Babafemi, S.Y. Kong, B. Šavija, Effect of recycled iron powder as fine aggregate on the mechanical, durability, and high temperature behavior of mortars, Materials (Basel). 13 (5) (2020) 1168.
[67] IS 13311 (Part 1), Method of Non-destructive testing of concret, Part 1: Ultrasonic pulse velocity, Bur. Indian Satandards. (1992) 1–7.
[68] K. Prakash A, J. Helena H, P. Oluwaseun Awoyera, F. Colangelo, Optimization of Mix Proportions for Novel Dry Stack Interlocking Concrete Blocks Using ANN, Adv. Civ. Eng. 2021 (2021) 1–15.
[69] M. John Robert Prince, B. Singh,, Bond behavior of deformed steel bars embedded in recycled aggregate concrete, Constr. Build. Mater. 49 (2013) 852–862, https://doi.org/10.1016/j.conbuildmat.2013.08.031.
[70] P.O. Awoyera, T.A. Nworgu, B. Shanmugam, K. Prakash Arunachalam, I. Mansouri, L.M.B. Romero, J.-W. Hu, Structural retrofitting of corroded reinforced concrete beams using bamboo fiber laminate, Materials (Basel). 14 (21) (2021) 6711.
[71] C. Shi, M. Liu, P. He, Z. Ou, Factors affecting kinetics of CO_2 curing of concrete, J. Sustain. Cem. Mater. 1 (2012) 24–33, https://doi.org/10.1080/21650373.2012.727321.
[72] L.K. Berger, R. L., J. F. Young,, Acceleration of hydration of calcium silicates.pdf, Nat. Phys. Sci. 240 (1972) 16–18.
[73] F. Pelisser, A. Vieira, A.M. Bernardin, Efficient self-compacting concrete with low cement consumption, J. Clean. Prod. 175 (2018) 324–332, https://doi.org/10.1016/j.jclepro.2017.12.084.
[74] M.S. Amin, S.M.A. El-Gamal, F.S. Hashem, Effect of addition of nano-magnetite on the hydration characteristics of hardened Portland cement and high slag cement pastes, J. Therm. Anal. Calorim. 112 (2013) 1253–1259, https://doi.org/10.1007/s10973-012-2663-1.